Quantum Nanosystems

Structure, Properties, and Interactions

Editor
Mihai V. Putz, PhD

Apple Academic Press

CRC Press
Taylor & Francis Group

QUANTUM NANOSYSTEMS

Structure, Properties, and Interactions

Edited by

Mihai V. Putz, PhD

Apple Academic Press

TORONTO NEW JERSEY

Apple Academic Press Inc.
3333 Mistwell Crescent
Oakville, ON L6L 0A2
Canada

Apple Academic Press Inc.
9 Spinnaker Way
Waretown, NJ 08758
USA

Printed in the United States of America on acid-free paper

International Standard Book Number-13: 978-1-926895-90-1 (Hardcover)

Library of Congress Control Number: 2014939543

Library and Archives Canada Cataloguing in Publication

Quantum nanosystems: structure, properties, and interactions/edited by Mihai V. Putz, PhD.

Includes bibliographical references and index.
ISBN 978-1-926895-90-1 (bound)

1. Nanostructures. I. Putz, Mihai V., author, editor

QC176.8.N35R42 2014 620'.5 C2014-902999-3

CHAPTER 2

DOI: 10.13140/2.1.1375.2324

INERTON FIELD EFFECTS IN NANOSYSTEMS

VOLODYMYR KRASNOHOLOVETS

CONTENTS

Abstract 60
2.1 Introduction 60
2.2 Submicroscopic Deterministic Concept 61
2.3 The Submicroscopic Behavior of Particles in Condensed Matter 74
2.4 Clusterization of Atoms/Molecules 77
2.5 Casimir Effect 92
2.6 Concluding Remarks 97
Keywords 98
References 98

ABSTRACT

The real physical space is derived from a mathematical space constructed as a tessellation lattice of primary balls, or a kind of superparticles. In the tessel-lattice particles are determined as local stable deformations. The motion of a particle generates a cloud of excitations around the particle, which were named *inertons*. An abstract construction of quantum mechanics known as the wave ψ-function is treated as a mapping of the real system "particle + its cloud of inertons." These inertons carry both the particle's inert and gravitational properties. It is shown how inertons manifest themselves experimentally, how they form clusters of particles in diluted cold gases, clusters of electrons, and how they are responsible for the Casimir effect. The inerton field, as well as the electromagnetic field, is a basic field of the universe. The inerton field is able to give a deeper insight into the fundamental nature of things playing an important role in quantum physics, chemical physics, biochemistry, biophysics, and condensed matter in general.

2.1 INTRODUCTION

Nanosystems approaching the fundamental microscopic length scales have demonstrated fundamentally new physical phenomena. New advances have been reached in many basic and enchanced areas of nanophysics, including diluted cold gases, carbon nanotubes, graphene, magnetic nanostructures, composite nanoparticles, transport through coupled quantum dots, spin-dependent electron transport phenomena, optical matrices with doped nanoparticles, molecular electronics and quantum information processing.

Usually new phenomena relating to nanosystems are associated with changes in electric and magnetic behavior of the systems studied in which electrical/magnetic polarizations are locally realized bringing new physical chemical properties, which can be applied to the electronics industry. Research of nanosystems is challenging as it enters the uncharted areas delimited by new nanoelectronic devices and fabrics. Such devices allow us to increase computational density up to 100 times, which extremely amplifies the capabilities of such systems in new areas of application and markets. New dynamic properties revealed in nanosystems enable the possibilities of nano-engines, nano-pumps and nano-propellors with advantages in distinctive sensors, biomedicine and energy savings and in sustainable development in general.

At the same time, in some peculiar situations some nanosystems unveil such new properties that they cannot be directly accounted for by conven-

tional electromagnetism and quantum mechanical laws. To such systems with special properties, in which peculiar quantum fluctuations are realized, belong those that manifest the so-called Casimir effect [1–4], an attractively interacting ensemble of ultracold bosons at negative temperature that is stable against collapse for arbitrary atom numbers [5]; an electron droplet (an aggregation of about 10^{10} electrons in one cluster) [6–12].

In this chapter, the submicroscopic deterministic concept is revealed in detail and its connection to the conventional quantum mechanical formalism is demonstrated. In the next sections unusual effects uncovered in nano- and submicroscopic systems ensue from the submicroscopic standpoint, namely, the effects incorporating quasi-particles named *inertons*, carriers of the inerton field, which, as is shown is a basic physical field of Nature.

2.2 SUBMICROSCOPIC DETERMINISTIC CONCEPT

A sub microscopic approach can be considered as the further development of conventional quantum mechanics, which incorporates the theory of ordinary physical space.

2.2.1 PHYSICAL SPACE

The term **space** is used somewhat differently in different fields of study. In physics **space** is defined via measurement and the standard space interval, called a standard meter or simply meter, is defined as the distance traveled by light in a vacuum per a specific period of time and in this determination the velocity of light is treated as constant. In microscopic physics, or quantum physics, the notion of **space** is associated with an "arena of actions" in which physical processes and phenomena take place. And this arena of actions we feel subjectively as a "receptacle for subjects." The measurement of **physical space** has long been important.

This "arena of actions" can be completely formalized, because fundamental physical notions (particle, mass, wave ψ-function, etc.) and interactions can be derived from pure mathematical constructions.

It is interesting to read Vernadsky's work who back in 1920–1930s introduced the notion of *noosphera* (from Greek *nous*—mind and *sphaira*—ball): a sphere of the arena of interaction between people and nature. In particular, he mentioned that Helmholtz probably was the first who noted that geometric space did not embrace all of empirically studied space, which Helmholtz called **physical space**; Helmholtz distinguished physical space from geomet-

ric space, as possessing its own properties, such as right-handedness and left-handedness; besides, Poincaré observed that geometry could not have been developed without solids [13]. Further Vernadsky notes: "In discussing the state of space, I will be dealing with the state of empirical or physical space, which has only in part been assimilated by geometry. Grasping it geometrically is a task for the future." Vernadsky introduced such notion as *the state of space*, which in his opinion has to be closely connected with the concept of a physical field, which plays such an important role in contemporary theoretical physics.

Researchers working in the realm of quantum gravity tend to believe that the real space has a cellular structure at the Planck scale. For instance, in the case of loop quantum gravity, basic excitations of the gravitational field are arbitrary and they can describe the quantum spacetime directly at the Planck scale, where the geometry comes by "quanta."

Models of a spin-network in quantum gravity are realized as a one-dimensional graph; spin foams generalize spin networks where instead of a graph one uses a higher-dimensional complex. Such geometry of spacetime corresponds to a kind of a lattice [14]. A "Planck-Lattice," a spacetime cubic lattice with the lattice constant equals to the Planck length $\ell_{\mathrm{P}} \cong 10^{-35}$ m models a ground state of quantum gravity of Wheeler's spacetime foam [15].

Granular space and the problem of large numbers – how many spatial cells may a canonical particle include – have recently been discussed in a simple way [16]. Wilczek says about space the following [17]: "…this is the effervescent Grid… Matter is not what it used to be. It consists of small, more-or-less stable patterns of disturbance in the Grid… Usually the metric field is taken to be fundamental, but in many ways it resembles a condensate, and that view of it may become important… What we ordinarily call matter consists of more-or-less stable patterns of excitation in the Grid, which is more fundamental. At least, that's how things look today."

All this means that **physical space** is a peculiar substrate that is subject to certain laws, which as has been seen below, are purely mathematical. Such a view allows us to completely remove any subjectivity and all the figurants of fundamental physical processes will be 100% defined. So, we can elucidate those something's that form a primordial physical substrate and determinate its mathematical properties.

Modern quantum theories wish to combine all fundamental interactions in a unified theory—*the theory of everything*. However, doing so the theory of everything rests on complete undetermined basic notions, such as mass, particle, charge, lepton, quark, Compton wavelength, de Broglie wavelength,

particle-wave, spin, etc. Moreover, the notion of space in which all physical processes occur is also beyond understanding, though the review above illustrates a gradual trend of the researchers to a fine-scale morphology that has to incorporate particles.

How can the situation be clarified? Can we start from *the theorem of something*? Then, having defined basic physics notions, we will be able to pass on to the construction of the theory of everything.

Bearing in mind an idea to build fundamental physics based on mathematical space, we first of all have to answer the question: What is space from the mathematical point of view? Basing on classical mathematics we may start from nothing – a flat space that does not manifest itself. How does real physical space appear? The flatness of the original mathematical space points to the fact that the Poisson brackets and any other forms of noncommutative features should be absent in such a space. In particular, the Heisenberg's uncertainty principle also becomes an alien for the ordinary flat space. This is what tells us the fundamental mathematics…

Mathematical space, as dealing with the notions of *measure*, *distances* and *dimensionality* in a broad topological sense was analyzed and constructed by Michel Bounias [18]. The major results of this work (for the case of totally topologically ordered space) are as follows.

The Jordan and Lebesgue measures involve respective mappings (I) and (M) on spaces which must be provided with operations $\cap, \cup$ and C. In spaces of the R^n type, tessellation by balls is involved, which again demands a distance to be available for the measure of diameters of intervals. Thus, since the intervals can be replaced by topological balls, the evaluation of their diameter still needs an appropriate general definition of a distance. A space E is ordered if any segment owns an infinum and a supremum. Therefore, a distance *d* between A and B is represented by the relation

$$d(\mathrm{A},\ \mathrm{B}) \subseteq \mathrm{dist}(\inf \mathrm{A},\ \inf \mathrm{B}) \cap \mathrm{dist}(\sup \mathrm{A},\ \sup \mathrm{B}) \tag{1}$$

with the distance evaluated through either classical forms or even the set-distance $\Delta(\mathrm{A},\mathrm{B})$. Any topological space is metrizable as provided with the set-distance Δ as a natural metrics. All topological spaces are kinds of metric spaces called "delta-metric spaces." Distance $\Delta(\mathrm{A},\mathrm{B})$ is a kind of an intrinsic case $\left[\Lambda_{(\mathrm{A},\mathrm{B})}(\mathrm{A},\mathrm{B})\right]$ of $\Lambda_{\mathrm{E}}(\mathrm{A},\mathrm{B})$ while the latter is called a "separating distance." The separating distance also stands for a topological metrics. Hence, if a physical space is a topological space, it will always be measurable.

A fundamental segment (A, B) and intervals $L_i = [A_i, A_{(i+1)}]$ allow one to determine similarity coefficients for each interval by $\rho_i = \text{dist}(A_i; A_{(i+1)}) = \text{dist}(A, B)$.

The similarity exponent of Bouligand (e) is such that for a generator with *n* parts:

$$\sum_{i \in [1, n]} (\rho_i)^e = 1 \tag{2}$$

Then, when 'e' is an integer, it reflects a topological dimension

$$e \approx \text{Log } n/\text{Log } \rho, \tag{3}$$

which means that a fundamental space E can be tessellated with an entire number of identical balls B exhibiting a similarity with E, upon coefficient *r*.

The measure of the size of tessellating balls as well as that of tessellated space, with reference to the calculation of their dimension is determined through Eqs. (2) and (3). A space may be composed of members, such that not all tessellating balls have identical diameter. Also a ball with two members would have a more complicated diameter. Thus a measure should be used as a probe for the evaluation of the coefficient of size ratio needed for the calculation of a dimension [18].

It is generally assumed [19] that some set does exist. This strong postulate was reduced to the axiom of the existence of the empty set [18]. Supplementing the empty set (Ø) with some operations and rules allowed us to construct a magma, which became an initiating polygon for a spatial lattice.

Recall that in abstract algebra a magma is defined as a set M supplied with a single binary operation interpreted and described usually (but not always) as a form of multiplication "·" and this binary operation is closed by definition. So, a magma is a set S in which the operation "·" forwards any two elements a, b to another element $a \cdot b$. To qualify as a magma, the set and operation (M, ·) must satisfy the magma axiom: For all a, b in M, the result of the operation $a \cdot b$ is also in M.

So, following ordinary algebraic canons, we [18] in fact could show that providing the empty set (Ø) with operations ($\in$, $\subset$) as the combination rules with the property of complementarity (C) results in the definition of a magma without violating the axiom of foundation if the empty set is seen as a hyperset that is a nonwellfounded set. The magma was defined as $\varnothing^{\varnothing} = \{\varnothing, \mathbf{c}\}$ and it was proved that such construction with the empty hyperset and the axiom of

availability is a fractal lattice an these features indeed characterize a fractal object [20].

Writing $\varnothing^{\varnothing}$ denotes that the magma reflects the set of all self-mappings of $(\varnothing)$, which emphasizes the forthcoming results. The space constructed with the empty set cells is a Boolean lattice $S(\varnothing)$ and this lattice is provided with a topology of discrete space. The magma of empty hyperset is endowed with self-similar ratios.

Such a lattice of tessellation balls was called a *tessel-lattice* [18, 21]. The magma of empty hyperset is a fractal tessel-lattice.

An abstract tessel-lattice of empty set cells accounts for a primary substrate in a physical space [21, 22]. Space-time is represented by ordered sequences of topologically closed Poincaré sections of this primary space. These mappings are constrained to provide homeomorphic structures serving as frames of reference in order to account for the successive positions of any objects present in the system. Mappings from one to the next section involve morphisms of the general structures, standing for a continuous reference frame, and morphisms of objects present in the various parts of this structure. The combination of these morphisms provides space-time with the features of a nonlinear generalized convolution (and then the process of motion appears as a stack of serial slices, that is, Poincaré sections, which resembles a customary movie). Discrete properties of the lattice allow the prediction of scales at which microscopic to cosmic structures should occur.

The fundamental metrics of space-time is represented by a convolution product where the embedding part D4 is described by the following relation:

$$\mathrm{D4} = \int\left(\int_{d\mathrm{S}} (d\mathbf{x}\cdot d\mathbf{y}\cdot d\mathbf{z}) * d\,\Psi(w)\right) \tag{4}$$

where dS is an element of space-time, and $d\,\Psi(w)$ a function accounting for the extension of 3D coordinates up to the 4th dimension timeless space through convolution (*) with the volume of space. Thus fractality of space manifests itself through changes in the dimension of geometrical structures. For example, the dimension of a curve exceeds 1D and falls in the interval between 1D and 2D; for a volumetric object the dimension may lay between 3D and 4D.

Thus the real physical space is organized as the tessel-lattice of primary topological balls. The existence of such lattice stands for the universe substrate (or "space"). In a degenerate state the size of a ball, which plays the role of a lattice's cell, is associated with the Planck length ℓ_{p}. Deformations of

primary cells by exchange of empty set cells allow a cell to be mapped into an image cell in the next section as far as mapped cells remain homeomorphic.

The tessel-lattice is specified with quanta of distances and quanta of fractality [21, 22]. The sequence of mappings of one into another structure of reference (e.g., elementary cells) represents an oscillation of any cell volume along the arrow of physical time.

A lattice that includes a set with neither members nor parts accounts for both relativistic space and quantic void, since: (i) the concept of distance and the concept of time have been defined on it, and (ii) this space holds for a quantum void since on the one hand it provides a discrete topology with quantum scales, and on the other hand it contains no "solid" object that would stand for a given provision of physical matter.

When a fractal transformation is involved in exchange of deformations between cells, there occurs a change in the dimension of the cell and the homeomorphism is not conserved [21]. Then the fractal kernel (a local deformation of the tessel-lattice) stands for a "particle" and the reduction of its volume is compensated by morphic changes of a finite number of surrounding cells. These morphic changes represent a typical tension of the tessel-lattice around the deformed fractal kernel, that is, particle.

Since we have introduced a particle, we must provide it with physical properties. First of all this is mass: The mass m_A of a particulate ball A is a function of the fractal-related decrease of the volume of the ball:

$$m_A \propto (V^{\text{deg. cell}} / V^{\text{part}}) \cdot (\mathrm{e}_{\text{fract}} - 1)_{\mathrm{e}_{\text{fract}} > 1} \tag{5}$$

where $V^{\text{deg. cell}}$ is the typical average volume of a cell in the tessel-lattice in the degenerate state; V^{part} is the volume of the kernel cell of the particle; (e) is the Bouligand exponent, and $(\mathrm{e}_{\text{fract}} \quad 1)$ the gain in dimensionality given by the fractal iteration. Just a volume decrease is not sufficient for providing a ball with mass, since a dimensional increase is a necessary condition (there should be a change in volumetric fractality of the ball) [21, 22].

As follows from Eq. (5), mass appears as a deformation of a cell, that is, at the volumetric fractal contraction of the cell. This is typical for leptons and hence in the case of leptons $V^{\text{deg. cell}} / V^{\text{lepton}} > 1$ (the volume of the particle kernel is less than the volume of the original degenerate cell). In the case of quarks the situation is reciprocal: the quark's kernel cell has a volume bigger than the average volume of a degenerate cell, that is, $V^{\text{quark}} / V^{\text{deg. cell}} > 1$ [22].

Therefore, in the tessel-lattice a lepton is a contracted kernel-cell. Surrounding cells compensate this local deformation by morphic changes (a cell tension) forming a peculiar deformation coat with a radius identified with

the particle's Compton wavelength $\lambda_{\text{Com}} = h/(mc)$. Beyond the radius λ_{Com} there is no information about the particle. This hidden radius indeed manifests itself in the experiments on light scattering by particles, though in orthodox quantum mechanics the size of a canonical particle does not play a part in the theory.

In condensed matter physics the availability of a deformation coat is a typical situation. It emerges in a crystal lattice when a foreign particle or isotope defect arises in the solid (for example, small and big polarons); a similar situation occurs in a liquid (a solvate shell forms around an entered ion) and liquid crystal.

2.2.2 MECHANICS OF THE TESSEL-LATTICE

A local stable deformation in the tessel-lattice, that is, a volumetric fractal deformation of a cell of the tessel-lattice, can be treated as a massive particle. The motion of such particle occurs with the interaction with surrounding cells (Fig. 2.1). This situation is fundamentally different from what we have in Newtonian mechanics – because in the latter the particle moves without interacting with space.

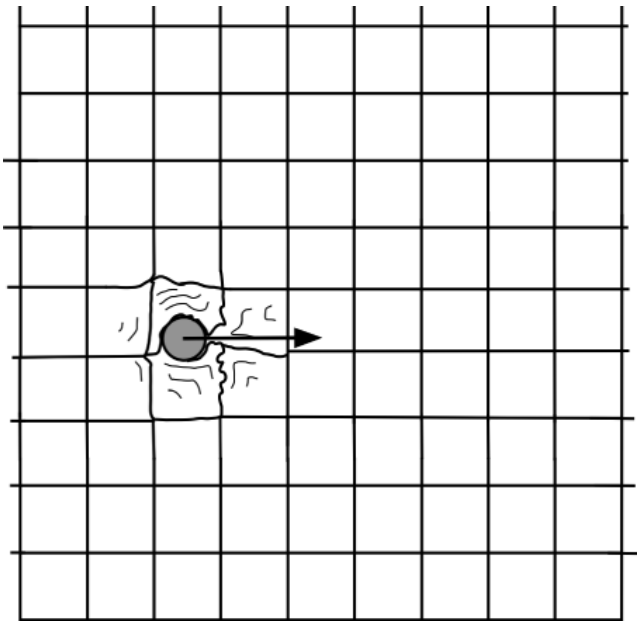

FIGURE 2.1 Motion of the local stable deformation in the tessel-lattice.

Motion of a particle in the tessel-lattice is accompanied by friction, which is obvious. The particle contacting oncoming cells of the tessel-lattice emits excitations, which finally has to stop the particle, as it loses energy. However, if these excitations are reabsorbed by the particle, it will continue to move ahead. No energy is lost in this interaction, that is, all excitations are reabsorbed by the particle and no friction heat is generated. Thus we may assume that a particle in the tessel-lattice moves rectilinearly in such a way that its velocity oscillates between the initial value υ_0 and zero, that is, during odd half a period the particle emits excitations and gradually loses the velocity and during the next even half a period it absorbs the emitted excitations gaining speed, and so on. These spatial excitations were named *inertons* [23, 24] since they reflect the inert properties of matter – a resistance on the side of space to a stimulation of the movement of the object. The principle of motion is shown in Fig. 2.2.

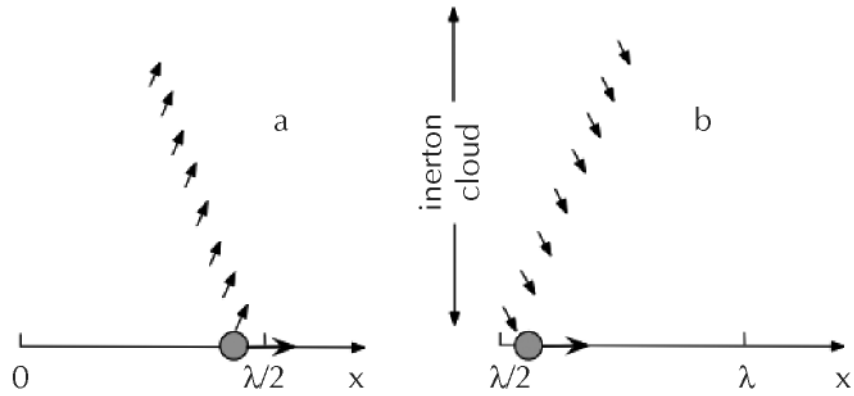

FIGURE 2.2 Motion of the particle in the tessel-lattice, which is accompanied with the emission of inertons. The moving particle periodically emits inertons in the odd part of its spatial period (in the section [0, λ/2], (a); and absorbs them in the second part of the spatial period (in the section [λ/2, λ], (b).

It is interesting that such a pattern of the motion embraces ideas of Poincarè and de Broglie on the principles of motion of canonical particles. Indeed, [25] pointed out that an electron is a singularity in the world ether and it should move surrounded by the ether excitations. De Broglie [26] instinctively put those excitations in order, such that the excitations became a wave guiding the particle (one can see this in Fig. 2.2b). However, in 1927 at the Fifth Solvay International Conference he was persuaded to the

probabilistic interpretation of quantum mechanics, which was suggested by Born in 1926 [27, 28]. Nevertheless, later on since 1952 [29]) was firmly searching for the double solution theory, which would be able to reinterpret the wave ψ-function so that it showed its physical interpretation rather than probabilistic discoloration.

The behavior of a particle in the tessel-lattice can be described by the following Lagrangian [23, 24, 30].

$$L = -m_0 c^2 \left\{ 1 - 1/(m_0 c^2) \left[m_0 \dot{x}^2 + \mu_0 \dot{\chi}^2 - 2\pi / T \sqrt{m_0 \mu_0}\, (x\dot{\chi} - \upsilon_0 \chi) \right] \right\}^{1/2} \qquad (6)$$

where m_0 is the particle's mass, x is its position; μ_0 is the mass of the excited cloud of inertons (excitations of the tessel-lattice associated with the field of inertia of the particle), χ is the position of the center mass of the cloud; $1/T$ is the frequency of collisions of the particle with the cloud of inertons; υ_0 is the initial velocity of the particle and c is the speed of light. This Lagrangian is constructed as an inner development of the so-called relativistic Lagrangian of a particle $L = -m_0 c^2 \sqrt{1 - \upsilon_0^2 / c^2}$.

The moving particle is rubbing against the tessel-lattice, which results in the appearance of the particle's cloud of inertons. But this is not a classic friction that stops the particle. Indeed, the Euler-Lagrange equations

$$d / dt\, (\partial L / \partial \dot{q}) - \partial L / \partial q = 0$$

for the particle ($q \equiv x$) and its inerton cloud ($q \equiv \chi$), which are based on the Lagrangian equation (the Eq. (6)), result in:

$$\frac{d^2 x}{dt^2} + \frac{\pi}{T} \frac{\upsilon_0}{c} \frac{dx}{dt} = 0 , \qquad (7)$$

$$\frac{d^2 \chi}{dt^2} - \frac{\pi}{T} \frac{c}{\upsilon_0} \left(\frac{d\chi}{dt} - \upsilon_0 \right) = 0 . \qquad (8)$$

The corresponding solutions to Eqs. (7) and (8) for the particle and the inerton cloud are:

$$\dot{x} = \upsilon_0 \cdot \left(1 - |\sin(\pi t / T)| \right) \qquad (9)$$

$$x = \upsilon_0 t + \lambda / \pi \cdot \left\{ (-1)^{[t/T]} \cos(\pi t / T) - \left(1 + 2[t / T] \right) \right\} , \qquad (10)$$

$$\chi = \Lambda / \pi \cdot |\sin(\pi t / T)|, \tag{11}$$

$$\dot{\chi} = (-1)^{[t/T]}\, c \cos(\pi t / T) \tag{12}$$

$$\lambda = \upsilon_0 T, \qquad \Lambda = cT \tag{13}$$

The Eqs. (9) and (10) show that the particle's velocity periodically oscillates and λ is the amplitude of the particle's oscillations along its path. In particular, λ is the period of oscillation of the particle's velocity that changes between υ_0 and zero. An oscillation of the particle's velocity is a very interesting feature of the tessel-lattice's mechanics (Fig. 2.3). The inerton cloud periodically leaves the particle and then comes back; Λ is the amplitude of oscillations of the cloud and *c* is the velocity of the cloud of inertons.

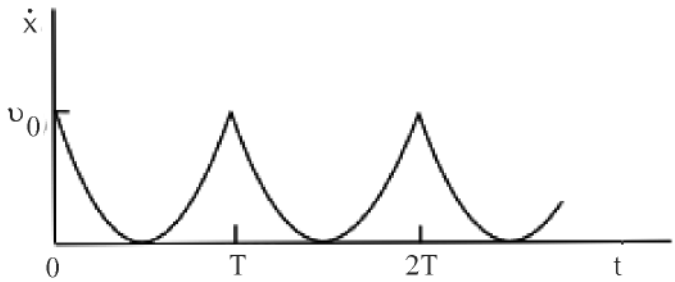

FIGURE 2.3 This is the graphical presentation of the solution (the Eq. (9)) for the behavior of the particle's velocity $\dot{X}$ as a function of time *t*. The time interval *T* of collisions of the particle with its inerton cloud plays the role of the period of the particle's velocity oscillations.

The Lagrangian (6) allows us to introduce an effective Hamiltonian of the particle, which describes its behavior relative to the center of inertia of the particle-inerton cloud system,

$$H_{\text{eff}} = p^2 / (2m) + m\left[2\pi / (2T)\right]^2 X^2 / 2 \tag{14}$$

where $m = m_0 / \sqrt{1 - \upsilon_0^2 / c^2}$. This is the harmonic oscillator Hamiltonian, which means that we can construct the Hamilton-Jacobi equation for a shortened action S_1 of the particle,

$$(\partial S_1 / \partial x)^2 / (2m) + m\left[2\pi / (2T)\right]^2 X^2 / 2 = E \tag{15}$$

where E is the energy of the moving particle. Introduction of the action-angle variables leads to the following increment of the particle action within the cyclic period $2T$,

$$\Delta S_1 = \oint p\, d\, x = E \cdot 2T \tag{16}$$

The Eq. (16) can be rewritten by using the frequency $\nu = 1/(2T)$. At the same time $1/T$ is the frequency of collisions of the particle with its inertons cloud. Allowance for $E = m\upsilon_0^2/2$ gets,

$$\Delta S_1 = m\upsilon_0 \cdot \upsilon_0 T = p_0 \lambda \tag{17}$$

where $p_0 = m\,\upsilon_0$ is the particle's initial momentum. If we equate the increment of action ΔS_1 per period to Planck's constant h, we obtain instead of Eqs. (16) and (17) the major de Broglie's relationships

$$E = h\nu, \qquad \lambda = h / p\,, \tag{18}$$

which form the basis of conventional quantum mechanics.

The Eq. (18) allow one to derive the Schrödinger equation [31]

$$-\frac{\hbar^2}{2m}\nabla^2 \psi(r,\, t) + V(r)\, \psi(r,\, t) = E\psi(r,\, t)\,. \tag{19}$$

The submicroscopic concept developed in the real space constructed as the tessel-lattice with the size of a cell equal to the Planck length operates with a particle and the particle's cloud of inertons. Conventional quantum mechanics, which was evolved in an abstract phase space on an atom scale, works with the wave ψ-function. These two approaches can be combined, as the inerton cloud of an entity, which is associated with the entity's field of inertia, is mapped into an abstract phase space of ordinary quantum mechanics in the form of a "mysterious" wave ψ-function (Fig. 2.4).

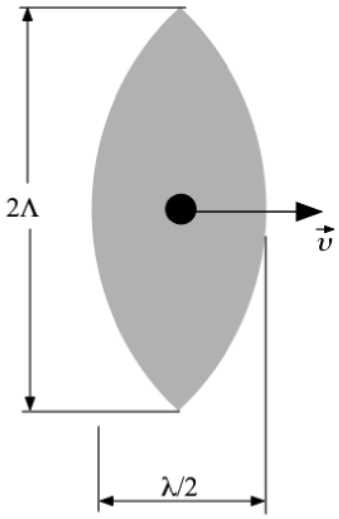

FIGURE 2.4 Moving particle with the velocity $\vec{v}$, which is surrounded by its cloud of inertons. An approximate size of such complicated system {particle + its inerton cloud} is determined by the cloud's amplitude Λ and the de Broglie wavelength λ. This complicated system determined in the real space is mapped to conventional quantum mechanics constructed in an abstract phase space as the particle's wave ψ-function.

Therefore, in the framework of the submicroscopic concept the cloud's inertons are a substructure of the matter waves. Inertons are field carriers – carriers of the field of inertia of the particle. They transfer mass and fractal properties from the particle to distant points of space. Why inertons emitted by a moving particle comes back to it? This is because the tessel-lattice is a reverberating substrate. (Of course these inertons may interference with other inertons and partly be absorbed by other objects, which correlate the behavior of the particle in question. This allows for entanglement.)

A range of space covered by the particle's inertons (i.e., particle's wave ψ-function) is specified by the amplitude of the inerton cloud,

$$\Lambda = \lambda c / \upsilon_0 , \tag{20}$$

which is spread in transversal directions from the particle's path; the particle's de Broglie wavelength λ is a section of the particle's path, the particle's amplitude; υ_0 is the initial velocity of the particle, and also the component of the velocity of the inerton cloud along the particle's path; c is the speed of light that is the velocity component of migrating inertons in the inerton cloud, which migrate transversal to the particle's path. If the particle is motionless, its

inertia and gravitation are restricted in the particle's deformation coat whose radius coincides with the particle's Compton wavelength $\lambda_{\text{Com}} = h/(mc)$ where m is the particle's mass.

In a macroscopic object (which is embedded in the tessel-lattice) local oscillations of entities generate inerton clouds that overlap, producing a set of harmonics of inerton waves [32, 33]. Moreover, long-wave inerton harmonics go far beyond the physical size of the object. These oscillating waves bear mass properties to a great distance away from the object. Oscillating waves mean that inertons emitted by the object return to it, which signifies that these inerton waves are standing spherical waves.

Solutions to standing spherical waves are characterized by the inverse dependence on the distance to the wave's front. The standing inerton wave results in a quasi-stationary mass potential field around the object with a mass M_0, which is subjected to spherical symmetry.

$$M \sim M_0 / r \tag{21}$$

This average mass field automatically results in the Newton's gravitational potential [34]

$$U = -GM_0 / r \tag{22}$$

Besides, the notion of a point mass, which is typical for general relativity, cannot be a real point but rather a small macroscopic object whose smallest radius can be estimated at around 1 μm.

The submicroscopic theory has been further developed for the interaction of massive objects. It was exhibited that the gravitational interaction between two objects should be described by a corrected Newton's law [35].

$$U = -G\frac{M_0 M_1}{r}\cdot\left(1+\frac{\dot{r}_{\tan}^2}{c^2}\right) \tag{23}$$

where $\dot{r}_{\tan}$ is the tangential velocity of a test mass M_1, which is in line with Poincaré's remark that an expression for the gravitational interaction should include the velocity of a moving object [25]. By using Eq. (23), the submicroscopic approach has successfully been applied to describe four macroscopic phenomena, which are treated as four classical tests for general relativity; they are: the motion of Mercury's perihelion, bending of a light ray by a star, the red shift of spectral lines [35, 32], and the Shapiro time delay effect [36].

Finally in this section, we mention that the submicroscopic approach allowed us to resolve successfully the big cosmological problem related to

so-called dark matter [37]. Standing inerton waves oscillate around the massive objects with the speed of light. They are those waves that induce the gravitational attraction between objects. In addition an overlapping of these standing oscillating inerton waves generates an elastic interaction between masses bringing them to a formation of clusters in which masses are characterized by both the Newtonian and elastic interaction. It is this elastic interaction that so far eluded researchers has been associated with the manifestation of dark matter.

The tessel-lattice also enables naturally the introduction of electric and magnetic charges and electromagnetic field [32, 38]

2.3 THE SUBMICROSCOPIC BEHAVIOR OF PARTICLES IN CONDENSED MATTER

The submicroscopic approach allows us to shed new light upon a number of well-known phenomena in condensed matter. This approach makes it possible to investigate how the quantum mechanical field (a substructure of the matter waves, that is, inertons, carriers of the particles' field of inertia) determines the collective behavior of atoms. In submicroscopic mechanics, the momentum p of a particle is decomposed to the mass m and the velocity υ and each of these parameters is characterized by its own behavior in the line of a particle's path. The whole particle path is subdivided by the particle's de Broglie wavelength λ. Along the section λ the particle velocity changes from υ to zero and is then again reinstated to υ, i.e. $\upsilon \to 0 \to \upsilon \to 0$ .. Owing to the emission and re-absorption of inertons by the particle, its mass also varies, $m \to 0 \to m \to 0$ …, but of course m does not disappear: the particle's mass state m is periodically passed to a local tension Ξ that is induced on the particulate cell: $\Xi \to 0 \to \Xi \to 0...$ (the tension is a displacement of the volumetric fractal deformation from its equilibrium state, periodically changing to a local tension of space). There is nothing extraordinary in such a behavior. An electric charge (e) moves in the same way along its path, which periodically is transformed to the magnetic monopole (g) state: $e \to g \to e \to g ...$ [32, 38].

Thus, the core of a moving particle is accompanied by a cloud of the particle's inertons ejected from the particle on its collisions with oncoming cells of the space tessel-lattice. In condensed media, atoms/molecules vibrate near their equilibrium positions. The crystal lattice is a good model to reveal major regularities in mass dynamics of condensed matter in general (a solid, liquid or gas) and that is why this model has been used to study the behavior of the

mass of atoms in the crystal lattice. In the crystal lattice the behavior of nodes is defined by the Lagrangian equation,

$$L_{\text{vibr.}} = \tfrac{1}{2}\sum_{\mathbf{n}}\left(m\,\delta\dot{r}_{\mathbf{n}}^{2} - \gamma\delta r_{\mathbf{n}}^{2}\right) \tag{24}$$

where $m_{\mathbf{n}}$ is the mass of the **n***th* node, $\delta r_{\mathbf{n}}$ is the deviation of this node from its equilibrium position and γ is the force constant. It is well known that based on the Lagrangian equation (the Eq. (24)), the Euler-Lagrange equations can be constructed, which completely determine the dynamics of the nodes.

Since massive nodes vibrate near their equilibrium positions, that is, are in motion, they emit and reabsorb clouds of inertons. Therefore inertons periodically remove a part of the mass from vibrating nodes and subsequently bring it back. Such behavior can be described in terms of the Lagrangian equation (the Eq. (25)) (for simplicity of consideration we consider an one-dimensional lattice), which is similar in form to the Eq. (24) but is different in dimension, as its variables are masses [33].

$$L_{\text{mass}} = \sum_{\mathbf{n}}\left\{\tfrac{1}{2}\dot{m}_{\mathbf{n}}^{2} - \tfrac{\pi}{2\bar{T}}\left(\dot{m}_{\mathbf{n}}\mu_{\mathbf{n}} + \dot{m}_{\mathbf{n}+\mathbf{g}}\mu_{\mathbf{n}}\right) + \tfrac{1}{2}\dot{\mu}_{\mathbf{n}}^{2}\right\} \tag{25}$$

where $m_{\mathbf{n}}$ and $\mu_{\mathbf{n}}$ are variations of mass of **n***th* node and its cloud of inertons, respectively, which occur due to the overlapping of inerton clouds of neighboring nodes; $\boldsymbol{g}$ is the lattice vector; $\bar{T}$ is the period of collision of the mass located in the **n**th node with its inerton cloud. The dot over mass means the derivative in respect to the time *t* treated as a natural parameter.

Instead of variables $m_{\mathbf{n}}$ and $\mu_{\mathbf{n}}$ we may pass on to collective variables $\Phi_{\mathbf{k}}$ and $\phi_{\mathbf{k}}$ by rules

$$m_{\mathbf{n}} = \tfrac{1}{\sqrt{N}}\sum_{\mathbf{k}}\Phi_{\mathbf{k}}\,e^{i\,\mathbf{k}\,\mathbf{g}},\ \mu_{\mathbf{n}} = \tfrac{1}{\sqrt{N}}\sum_{\mathbf{k}}\varphi_{\mathbf{k}}\,e^{i\,\mathbf{k}\,\mathbf{g}} \tag{26}$$

Substituting Eq. (26) into Eq. (25), we obtain:

$$L_{\text{mass}} = \tfrac{1}{N}\sum_{\mathbf{k}}\left\{\tfrac{1}{2}\dot{\Phi}_{\mathbf{k}}\dot{\Phi}_{-\mathbf{k}} - \tfrac{\pi}{2\bar{T}}\left(1+\cos\mathbf{k}\mathbf{g}\right)\dot{\Phi}_{\mathbf{k}}\,\varphi_{-\mathbf{k}} + \tfrac{1}{2}\dot{\varphi}_{\mathbf{k}}\,\dot{\varphi}_{-\mathbf{k}}\right\}. \tag{27}$$

The Euler-Lagrange equations for the variables $\Phi_{\mathbf{k}}$ and $\phi_{\mathbf{k}}$ become

$$\ddot{\Phi}_{\mathbf{k}} - \omega(k)\,\dot{\varphi}_{-\mathbf{k}} = 0 \tag{28}$$

$$\ddot{\varphi}_{\mathbf{k}} + \omega(k)\,\dot{\Phi}_{\mathbf{k}} = 0 \tag{29}$$

where we designate $\omega(k) = \frac{\pi}{2\bar{T}}\left(1+\cos(\mathbf{kg})\right)$.

Periodical solutions to Eqs. (28) and (29), which satisfy the physical characteristics of the system of varying masses, can be chosen as follows:

$$\Phi_{\mathbf{k}} = \Phi_0 + \Phi_1 \cos\left(\omega(k)\, t\right), \tag{30}$$

$$\phi_{\mathbf{k}} = -\Phi_1 \cos\left(\omega(\mathbf{k})\, t\right) \tag{31}$$

where parameters Φ_0 and Φ_1 are proportional to the rest mass of the system's particles and the mass of their inerton clouds, respectively, and inversely proportional to the square root of the total number of particles $N^{-1/2}$. The mentioned arguments point out that the variables Φ_k and ϕ_k represent collective massive excitations in the lattice: Φ_k describes collective mass excitations of the nodes of the lattice; ϕ_k characterizes the mass field of inertons that fill the entire space between the nodes in the lattice, like dust.

It should be emphasized that these mass excitations are completely independent from the phonons of the lattice, because phonons are associated with collective changes of positions of nodes (atoms). Mass excitations described by the variable Φ_k represent the collective mass state of nodes at the moment *t* and the variable ϕ_k depicts the collective state of the total inerton cloud of the lattice.

The amplitude δm of oscillations of the **n***th* node's mass can crudely be estimated as a ratio of the dispersion of the **n**th node's inerton cloud at the maximal distant object ($r = \Lambda$) and the nearest node ($r = g$).

$$\delta m \approx m_{\mathbf{n}} \frac{g}{\Lambda} \sim 10^{-4} m_{\mathbf{n}} \tag{32}$$

where Λ is the amplitude of the inerton cloud of the **n***th* node. In accordance with Eq. (24), the mentioned amplitude is related to the node's de Broglie wavelength, $\lambda_{\mathbf{n}} \equiv \delta r_{\mathbf{n}}$, the node's velocity υ (sound velocity, as the node participates in acoustic vibrations) and the inerton velocity in the lattice can be equal to the velocity of light *c*; then

$$\Lambda_{\mathbf{n}} = \delta r_{\mathbf{n}} \frac{c}{\upsilon} \geq \delta r_{\mathbf{n}} \cdot 10^5 \ \sim \ 10^4 g\,. \tag{33}$$

Thus, we can see that in a solid we have an additional physical field, which is the inerton field that so far has not been practically taken into account. In fact, vibrations of atoms result in a series of acoustic waves. But the space between atoms is filled with inertons, which appear owing to the interaction

of vibrating atoms with the space organized as the tessel-lattice. Overlapping of inerton clouds and the mobility of atoms, which is the source of these inertons, bring about the formation of inertons waves (with their own harmonics) in the solid as well.

2.4 CLUSTERIZATION OF ATOMS/MOLECULES

[39] studied the behavior of a system of particles with a different character of interaction. The approach makes it possible to describe systems of interacting particles by statistical methods taking into account their nonhomogeneous spatial distribution, that is, cluster formation. For these clusters are evaluated: their size, the number of particles in a cluster, and the temperature of phase transition to the cluster state. The approach developed is very suitable for examination of nanosystems, it allows one to study pair interaction potentials between molecules forming a nanoparticle and also the interaction between nanoparticles. Among these interactions the inerton interaction is also is present, which brings quite new and sometimes unexpected properties to the systems studied.

2.4.1 FORMALISM OF CLUSTER FORMATION

We may start from the construction of the Hamiltonian for a system of interacting particles. The energy for such a system can be written in the general form [40],

$$H = H_0 - \tfrac{1}{2}\sum_{\mathbf{r},\mathbf{r}'} V^{\text{att.}}_{\mathbf{r}\mathbf{r}'}\; c(\mathbf{r})\,c(\mathbf{r}') + \tfrac{1}{2}\sum_{\mathbf{r},\mathbf{r}'} V^{\text{rep.}}_{\mathbf{r}\mathbf{r}'}\; c(\mathbf{r})\,c(\mathbf{r}')\,. \tag{34}$$

Particles occupy knots in Ising's lattice described by the radius vectors $\mathbf{r}$ and $\mathbf{r}$, and the filling number for the ith knot $c_i(\mathbf{r}) = \{0, 1\}$. If the potentials $V^{\text{att.}}_{\mathbf{r}\mathbf{r}}$, $V^{\text{rep.}}_{\mathbf{r}\mathbf{r}} > 0$, the second term (comprising $V^{\text{att.}}_{\mathbf{r}\mathbf{r}}$) in the right-hand side of the Hamiltonian (34) corresponds to the effective attraction and the third term (comprising $V^{\text{rep.}}_{\mathbf{r}\mathbf{r}}$) conforms to the effective repulsion. This allows us to represent the Hamiltonian (34) in the form typical for the model of ordered particles, which is characterized by a certain nonzero order parameter,

$$H(n) = \sum_{s} E_s\, n_s - \tfrac{1}{2}\sum_{s,s'} V^{\text{att.}}_{ss'}\; n_s\, n_{s'} + \tfrac{1}{2}\sum_{s,s'} V^{\text{rep.}}_{ss'}\; n_s\, n_{s'}. \tag{35}$$

Here E_s is the additive part of the particle energy (the kinetic energy) in the *s*th state. So, we have two terms for particle/molecular potential: the attraction and the repulsion components. So, in the Hamiltonian (35) the potential $V_{ss}^{\text{att.}}$ represents the paired energy of attraction and the potential $V_{ss}^{\text{rep.}}$ is the paired energy of repulsion. The potentials take into account the effective paired interaction between particles/molecules located in states s and s'. The filling numbers n_s can run only two values: 1 (the *s*th knot is occupied) or 0 (the *s*th knot is not occupied). The signs before positive functions $V_{ss}^{\text{att.}}$ and $V_{ss}^{\text{rep.}}$ in the Hamiltonian (35) directly specify proper signs of attraction (minus) and repulsion (plus).

The statistical sum of the system of interacting particles,

$$Z = \sum_{\{n\}} \exp\left(-H(n)/k_{\text{B}}\Theta\right) \tag{36}$$

can be rewritten via the action $\tilde{S}$, which depends on three functions,

$$Z = \text{Re}\frac{1}{2\pi i}\int D\varphi \int D\psi \oint dz \exp\left[\tilde{S}(\varphi,\ \psi,\ z)\right]\cdot \tag{37}$$

The complicated function $\tilde{S}(\phi,\ \psi,\ z)$ was evaluated for extremum [39]. The most stable solution appears when all particles are distributed by clusters, especially if each cluster includes the same number of particles. In this case the action for a cluster of *N* quantum particles becomes

$$S \approx \tfrac{1}{2}\{a(N) - b(N)\}\cdot N^2 \tag{38}$$

where the functions *a* and *b* are defined as follows:

$$a = 3\int_1^{N^{1/3}} V^{\text{rep.}}(g\,x)\,x^2\,dx/(k_{\text{B}}\Theta), \tag{39}$$

$$b = 3\int_1^{N^{1/3}} V^{\text{att.}}(g\,x)\,x^2\,dx/(k_{\text{B}}\Theta) \tag{40}$$

where *g* is the lattice constant.

Having known the explicit form of the action (38), one can derive the equation for the number of particles combined in a cluster: $\partial S/\partial N = 0$, which in addition requires holding of the inequality $\partial^2 S/\partial N^2\,|_{N=N_{\text{in cluster}}} > 0$.

The formalism described by Eqs. (38)–(40) can be applied to many different physical systems in which particles exhibit interaction. In particular, we described the behavior of electrons on a liquid helium surface; particles interacting by the shielding Coulomb potential, which are found under the influence of an elastic field; and gravitating masses with the Hubble expansion [39].

The formalism Eqs. (38)–(40) was used at studies of several other physical systems, which directly relate to the subject of the present paper.

2.4.2 "FROZEN" MOLECULES

The formalism proposed by Krasnoholovets and Lev [39] allows one to exam a possible cluster formation in a gas, liquid or solid. For the clusterization one needs two pair potentials that consist of a short-range repulsion and a longer-range attraction (or vice versa). In particular, for molecular systems these are potentials of Morse, Lennard-Jones and Buckingham (*see*, for example, Ref. [41]), which respectively look as follows:

$$V(r) = D_0 \cdot \left(e^{-2\alpha(r-r_0)} - 2e^{-\alpha(r-r_0)} \right),$$

$$V(r) = 4\varepsilon \cdot \left[\left(\frac{\sigma}{r} \right)^{12} - \left(\frac{\sigma}{r} \right)^{6} \right], V(r) = Ae^{-\alpha r} - \frac{B}{r^6}. \qquad (41)$$

However, following the general scheme presented in Eqs. (37)–(40), we reveal that for these three potentials the equation $\partial S / \partial N = 0$ does not have a solution in which $N >> 1$. In other words, it seems no clusters can be formed in molecular systems.

Notwithstanding this circumstance, the submicroscopic concept allows one to investigate how clusters arise in molecular systems. The problem of cluster formation is solved if we take into consideration vibrations of atoms/molecules near their equilibrium positions. In fact an entity in condensed matter experiences local vibrations that exist even at the absolute zero temperature, which is called the zero point energy.

Therefore, let us try to introduce an additional attracting potential, $\frac{1}{2} m \omega^2 \delta r^2$, where the amplitude δr of oscillations plays the role of the de Broglie wavelength of the vibrating entity. This expression can be rewritten as $\frac{1}{2} \gamma \delta r^2$. Such potential is extremely important, because owing to these oscillations the vibrating entity emits and absorbs its inertons, as has been described in the previous sections. Emitted inerton clouds overlap with similar

inerton clouds emitted by other entities, which results into the inerton interaction in the physical system. The inerton interaction is additional to the pair interaction of electric nature, which reflects the molecular potentials (41) (and similarly the inerton interaction emerges in systems of magnetically interacting atoms and ions).

Let us examine a model system of N molecules interacting through the Lennard-Jones pair potential taking into account the inerton interaction $\frac{1}{2}\gamma\delta r^2$ between molecules. The attraction part of the pair potential is:

$$V_{\text{att}}(gx) = \frac{V_0}{x^6} - \tfrac{1}{2}\gamma(\delta r)^2 x^2 \tag{42}$$

and the repulsion part

$$V_{\text{rep}}(gx) = \frac{V_0}{x^{12}}. \tag{43}$$

Here, on the right hand side of Eq. (42) in the first term the distance r from the node to a distant point is written as $r = gx$ and in the second term the amplitude of oscillations is depicted as $x\delta r$, where g is the lattice constant, δr becomes a parameter and x is the dimensionless variable that describes the distance. On the right hand side of Eq. (42) we also introduce the dimensionless variable x for the distance.

Note in the formalism described above, Eqs. (34)–(40), the sign describing attraction and repulsion is taken out of the values of V_{att} and V_{rep}; that is way the right hand side in the Eq. (42) has the opposite sign to the attraction [37]. In the case of a classical system of interacting particles the action looks as follows [33].

$$S \approx 2[a(N) - b(N)]N + N\ln\xi \tag{44}$$

where the functions a and b are determined in Eqs. (39) and (40), respectively.

For the potentials (the Eqs. (42) and (43)), the action (the Eq. (44)) has the form

$$S = -\tfrac{4}{3}\frac{V_0}{k_{\text{B}}\Theta}N + \tfrac{3}{5}\frac{\gamma\delta r^2}{k_{\text{B}}\Theta}N^{8/3} + N\ln\xi \tag{45}$$

and the equation for the number of molecules in a cluster $\partial S/\partial N = 0$ results in the solution (if we neglect the contribution on the side of the fugacity ξ)

$$N \approx \left(\frac{5}{6} \frac{V_0}{\gamma \delta r^2} \right)^{3/5} \tag{46}$$

The dependence of N as a function of δr is shown in Fig. 2.5. Thus the appearance of fractal clusters is governed by local vibrations of entities in condensed media. In particular, we can see the smaller δr, the larger N. However, this is possible only when the amplitude δr of oscillations of particles near their equilibrium positions begins to drop, that is, becomes less than approximately 10^{-11} m (Fig. 2.5).

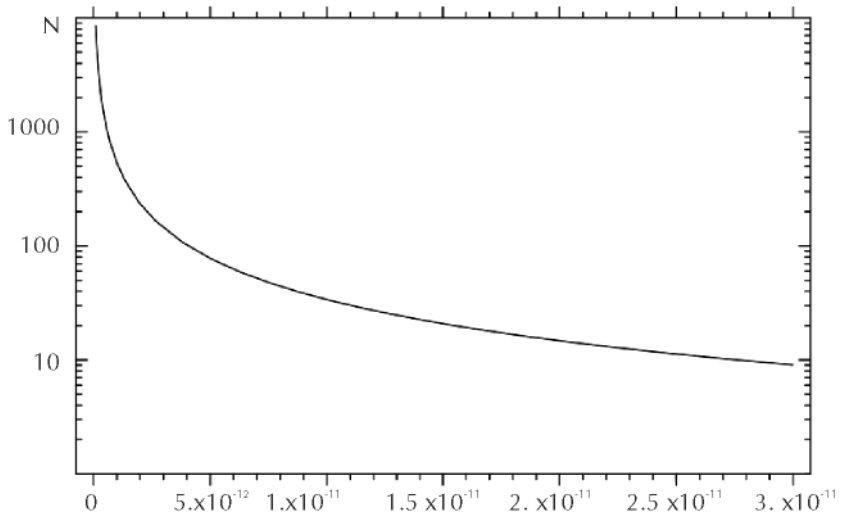

FIGURE 2.5 Numerical solution N versus δr (46). Values of the parameters are $V_0 = 4.25 \times 10^{-20}$ J and the force constant $\gamma = 1$ N/m.

Clusterization of water through the possible influence of an inerton field was also examined [33].

An external inerton signal is able to drop δr even if the temperature does not decrease, which immediately increases the number N of molecules in the cluster (or brings to a cluster in the case when it initially did not exist due to the relatively large value of δr). Indeed, since the mass of entities oscillates together with their oscillating motion, any additional injection of mass in the form of inertons causes absorption of an extra mass leading to the appearance

of a mass defect (or surplus defect) Δm in each irradiated entity. Hence, the amplitude of the entity's vibrations decreases:

$$\delta r = h/(m\upsilon) \rightarrow \delta r' = h/[(m+\Delta m)\upsilon], \ \delta r > \delta r' \tag{47}$$

The phenomenon of diminution of the amplitude of the entity's vibrations in a condensed matter is similar to decreasing the temperature: the lower the temperature, the lower the amplitude of vibrations. However, the temperature does not change. The phenomenon is stipulated by weighting of atoms, $m \rightarrow m + \Delta m$. The relaxation time, that is, return of the atom's mass to the initial state, $m + \Delta m \rightarrow m$, is very long. The relaxation time lasts for days or even months, which means that classical thermodynamics requires a significant reconsideration, because it must be supplemented by the mass exchange. First attempts to introduce some changes to the thermodynamics potentials caused by the mass exchange have already been taken [42–45].

Typical changes in the viscosity of sorbent samples irradiated by an inerton field are shown in Fig. 2.6. The dynamic viscosity and the shear viscosity of the sample under consideration significantly depend on the exposure time in an inerton field, which is shown in Fig. 2.7 for measurements conducted approximately half an hour after the inerton irradiation. Samples of water irradiated by an inerton field demonstrate an increase in the water density from 1 to about 1.2 kg/L, which was registered by a hydrometer. This indicates a change in both the density and the viscosity of water processed with an inerton field. Liquid substances, gels, hand creams, ointments and similar substances after processing with an inerton field generated by our device (Fig. 2.8) become more fluid demonstrating a kind of a 'superfluidity'. In particular, the rate of penetration of hand creams through the skin increases 20–30%, which was measured by a special facility used in cosmetology.

In Fig. 2.9, one can see our inerton measuring device 'Rudra,' which was designed to measure the intensity and the spectrum of inertons in a range of frequencies from a few Hz to 100 kHz. Two types of the antenna were tested: a ferrite rod with a coil and a piezoceramic sensor. The electric scheme of the device is functioning on the basis of principles described in the present subsection. The antenna's atoms absorbing inertons move from their equilibrium positions trying to arrange short-lived clusters, which results in an induction of local magnetic/electric fields in the antenna. In its turn these local fields impact electrons in the electronic scheme. The generated electric current is further processed, transmitting the received information to an analog-to-digital converter. The Rudra device successfully functions even when its antenna is

screened with a metal box, though usual receivers of electromagnetic waves have not been able to catch signals being directed towards this metal box.

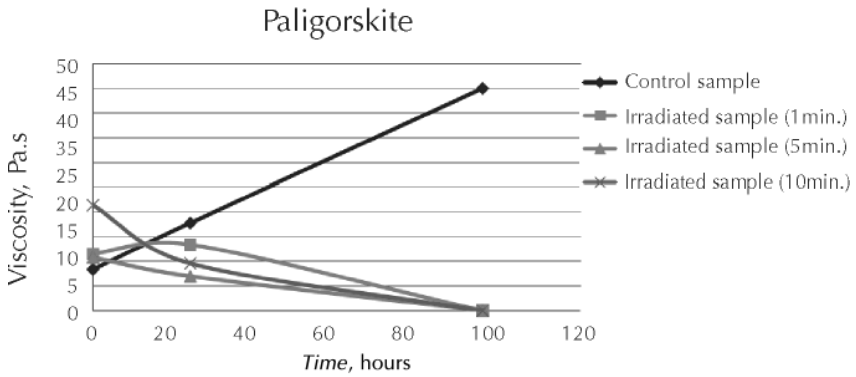

FIGURE 2.6 Behavior of the viscosity of samples of palygorskite (a magnesium aluminum phyllosilicate with formula $(Mg, Al)_2Si_4O_{10}(OH)\cdot 4(H_2O)$, a type of clay soil) irradiated with an inerton field. The viscosity of the control sample increases under atmospheric conditions with time, though the viscosity of the samples irradiated by the inerton field gradually decreases.

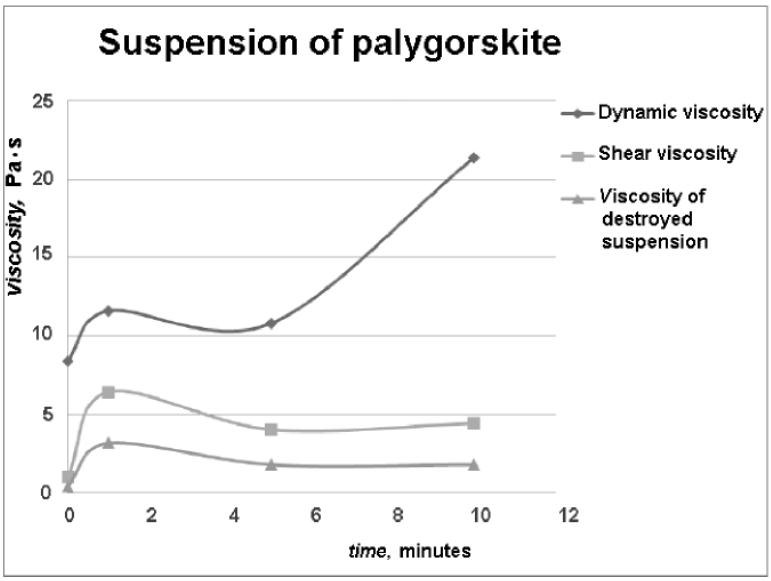

FIGURE 2.7 Viscosity versus time of inerton irradiation of an aqueous suspension of palygorskite.

FIGURE 2.8 Biaktor's laboratory batch unit Lx (http://biaktor.com). The device is intended for intensification of chemical physical reactions in liquid and gel substances.

FIGURE 2.9 Device 'Rudra' (interior and exterior) that measures inerton signals.

2.4.3 BOSE-EINSTEIN CONDENSATE

Although the gas cooling mechanism and the Bose-Einstein condensation of dilute gases were studied in detail, the submicroscopic approach allowed one to clarify subtle aspects of these phenomena [33]. Namely, the approach discloses

inner interactions and the organization of atoms in the Bose-Einstein condensate.

When atoms are cooled to a temperature when the de Broglie thermal wavelength $\lambda_{\rm th} = h/\sqrt{3mk_{\rm B}\Theta}$ is comparable to the mean distance g between atoms, atomic inerton clouds stop to overlap, but they still touch each other, which synchronizes the atoms. Namely, in such a case the $(\mathbf{n}-\mathbf{g})$th atom emits its inerton cloud that then is fully absorbed by the **n**th atom; the **n**th atom emits its own cloud of inertons, which then is fully absorbed by the $(\mathbf{n}+\mathbf{g})$th atom, etc. In other words, the coherent exchange of inerton clouds by the atoms when an inerton cloud emitted by one atom hops to the neighboring atom and is absorbed by it, we relate with the phenomenon of Bose-Einstein condensation.

Let us investigate whether the occurrence of clusters can be possible in a Bose-Einstein condensate. The action S for the ensemble of N interacting boson particles, which tend to clusterization with N particles in a cluster, has the form [33],

$$S \cong \left\{ \tfrac{1}{2}\left[a(N)-b(N)\right]N^2 - \ln(N+1) + N\,\ln\xi \right\} \tag{48}$$

where the functions a and b are determined in Eqs. (39) and (40), respectively, ξ is the rugosity, and in the action (the Eq. (48)) next two terms are preserved in contradistinction to the form (38). For simplicity, the repulsion potential can be taken in the form of Eq. (43). The attraction potential should include at least three terms: (i) the dispersion potential of interatomic interaction, which is usually written as $-C_6/r^6$; (ii) a potential formed by a trap, which can be modeled by a harmonic potential; and (iii) the harmonic potential caused by small spatial oscillations of atoms near their equilibrium positions, that is, inerton elastic interaction. So, the attraction and the repulsion potentials are

$$V^{\rm att.}(rx) = C_6/(rx)^6 - \tfrac{1}{2}\gamma_{\rm trap}\, r^2x^2 - \tfrac{1}{2}m\omega^2(\delta r)^2x^2, \tag{49}$$

$$V^{\rm rep.}(rx) = V_0/x^{12}, \tag{50}$$

where m is the mass of an atom, r is the distance between atoms, γ is the effective force constant of the trap, ω is the cyclic frequency of proper oscillations of an atom, δr is the appropriate amplitude and x is the dimensionless distance parameter.

Substituting potentials (the Eqs. (49) and (50)) into functions (the Eqs. (39) and (40)), respectively, we then construct the action (the Eq. (48)), which in the explicit form becomes

$$S = \left\{ \tfrac{1}{6} \frac{V_0}{k_B \Theta} N^2 - \tfrac{3}{6} \frac{C_6}{r^6 k_B \Theta} N^2 + \tfrac{3}{20} \frac{1}{k_B \Theta} \left(\gamma_{\text{trap}} r^2 + m \omega^2 \delta r^2 \right) N^{11/3} - \ln(N-1) + N \ln \xi \right\} \tag{51}$$

Proper oscillations of atoms, which are characterized by the frequency ω, are produced by the movement of the atoms. In other words, the origin of the frequency ω is produced by collisions of atoms with their inerton clouds [24, 30]: $\omega = 2\pi / 2T$ where T is the period of time between collisions of an atom and its inerton cloud (though in the present case we have to talk about collisions of the inerton cloud of an atom with the neighboring atom); the value of T is related to the amplitude δr of oscillations of an atom and its velocity υ, $1/T = \upsilon / \delta r$ (because the amplitude δr of oscillations of the atom is related to the atom's de Broglie wavelength λ). Since in the case of Bose-Einstein condensation we can put $\mu = 0$ for the chemical potential of atoms, the fugacity $\xi = 1$ and hence the last term in Eq. (51) reduces to zero.

The expression for the number of atoms combined in a cluster comes from the equation $\partial S / \partial N = 0$, or explicitly

$$N \cong \left(\tfrac{20}{33} \frac{3C_6 / r^6 - V_0}{\gamma_{\text{trap}} r^2 + m\omega^2 \delta r^2} \right)^{3/5}. \tag{52}$$

Here in Eq. (52) in the first approximation the numerator, that is, the difference between the attraction and repulsion energies at an equilibrium distance r of interacting atoms, can be put $3C_6 / r^6 - V_0 = 2.125 \times 10^{-20}$ J. For the case of cesium atoms whose mass $m_{\text{Cs}} = 2.207 \times 10^{-25}$ kg the amplitude δr of oscillations of an atom is associated with its de Broglie wavelength λ: $\delta r = \lambda = h / (m_{\text{Cs}} \upsilon)$. The trapping potential $\frac{1}{2} \gamma_{\text{trap}} r^2$ is the fitting parameter that can be chosen equal to 0, 2.5×10^{-29} and 2.5×10^{-28} J.

The oscillation of atoms is caused only by their thermal motion: $\upsilon \approx \upsilon_{\text{therm}} = \sqrt{3 k_B \Theta / m_{\text{Cs}}} \cong 3 \times 10^{-3}$ m/s where we put a typical temperature of Bose-Einstein condensate $\Theta = 50$ nK. So, $\delta r = \lambda_{\text{th}} = h / (m_{\text{Cs}} \upsilon_{\text{therm}}) \cong 10^{-6}$ m and then the cycle frequency of atom oscillations become $\omega = \pi \upsilon / \delta r \cong 9.43 \times 10^3$ s^{-1}. The abovementioned numerical values of the parameters allow the evaluation of the number of atoms that assemble in a Bose-Einstein cluster, as $N \sim 10^5$. The interatomic

interaction gathers dilute cold atoms to clusters. But the cluster state is realized when the absolute value of an attraction potential exceeds the thermal energy, $V^{\text{att.}} \geq k_{\text{B}}\Theta$. This inequality holds for the case calculated above: the attraction energy $\frac{1}{2} m_{\text{Cs}}\, \omega^2 \delta r^2 + \frac{1}{2}\gamma_{\text{trap}}\, r^2 \approx 1.7 \times 10^{-30}$ J exceeds the thermal energy $k_{\text{B}}\Theta \approx 7 \times 10^{-31}$ J.

Thus we have shown that the phenomenon of Bose-Einstein condensation of bosons, which by definition exists in momentum space, represents a stable cluster of these bosons in the real space.

An interesting paper has recently been published in which the authors [5] claim observation of ultracold bosons at negative temperature that is stable against collapse for arbitrary atom numbers. A negative temperature was derived in the framework of the following approach. The starting point was the Bose-Hubbard Hamiltonian

$$\hat{H} = -J \sum_{i,\, j} \hat{b}_i^{+} \hat{b}_j + \tfrac{1}{2} U \sum_i \hat{n}_i (\hat{n}_i - 1) + V \sum_i \hat{n}_i \mathbf{r}_i^2 \,, \tag{53}$$

which means, all cold atoms were distributed by sites of a lattice. In the Hamiltonian (the Eq. (53)) the first term describes a possible tunneling of atoms from one site to the other, the second term describes the attracting interaction between atoms, and the third term describes a cavity potential.

After some speculations in which Bose-Einstein condensation of atoms is reduced unreasonably to possible condensation of all atoms in one spatial point (though by the definition Bose-Einstein condensate is defined in momentum space), [5] indicate conditions for the existence of negative temperature: stable negative temperature states with bosons can exist only for attractive interactions and an antitrapping potential. This means that in the Hamiltonian (the Eq. (53)) the second term should be negative and the third term positive. Then at negative temperature high-energy states should be more occupied by the atoms than low-energy states.

In pursuit of a negative temperature [5] mixed together momentum space and the ordinary physical space. Besides, by using thermodynamic definition of temperature

$$1/\Theta = \partial \mathrm{S}/\partial E \tag{54}$$

where S is the entropy and E is the energy, they say the entropy should decrease with energy if high-energy states are more populated than low-energy ones.

It is obvious that the theoretical considerations [5] are devoid of any physical meaning. In fact, the Hamiltonian (53) is arranged in an abstract space related to a lattice whose sites are allied with the ordinary physical space. At the same time Bose-Einstein condensate is determined in momentum space, that is, all bosons have the same momentum and therefore the condensate cannot be associated with Eq. (53) to the full. By definition the notion of the entropy S is defined only for stationary states, though in the experiments of [5] they dealt with fast transitional processes. The energy E, which is part of the expression (54), also is not defined because in the Hamiltonian (the Eq. (53)) one can see only components of the potential energy, though the authors talk about the population of high-energy states, which is possible only via introduction of the kinetic energy. Why did other researchers who studied upper levels (second, third and so on) occupied by excited atoms not talk about negative temperatures? Moreover, all thermodynamic functions including the entropy S require a revision, which is associated with the presence of a mass field (the same as a temperature field, pressure field, etc.), as has been mentioned in the previous subsection. In addition, objections against the entropy as a fundamental thermodynamic potential, has recently substantiated by Zhang [46].

The above criticism allows us to reinterpret the interesting experimental data presented by Braun et al. [5] in the following way. Momentum distributions in the atomic cloud were measured for the cases of the rest atomic cloud and that excited by the laser beam. The measurement meant a series of captured images at intervals of a few milliseconds. Braun et al. distributed these images arranged in the final states of the atomic cloud between positive and negative temperatures. Images of the rest atomic cloud were related to positive temperatures and the images of excited atomic cloud were associated with negative temperatures.

If we look at the system of cold ^{39}K atoms studied by Braun et al. from the submicroscopic viewpoint and the mechanism of clustering described above, we will see that the Bose-Einstein condensate (or in other words the cluster state of cold atoms) is preserved as long as the kinetic energy of excited atoms remains less than the potential energy U in Eq. (52). Switching antitrapping potential, which decreases the trapping potential V in Eq. (52), creates excitations in the motion of atoms. Clearly, the temperature Θ should also be less than $|U$.

What is occurring in the cluster when some atoms become excited? First of all the anti-trapping potential partly diminishes the trapping potential $\frac{1}{2}\gamma_{\text{trap}} r^2$ in Eqs. (49) and (51). Besides, since the anti-trapping potential is distributed

in 3D space, we have to anticipate similar momentum distributions of atoms. Namely, the initially spherical cluster with the solution (the Eq. (51)) for the number of atoms must change the shape followed by the symmetry of anti-trapping potential. In fact, in the general case the variable N is subdivided into N_x, N_y and N_z. The corresponding changes will appear in expressions for the functions $a(N)$, $b(N)$ and also the action S (the Eq. (51)). Then the final solution for the number of atoms in a cluster will represent three different expressions along the axes X, Y and Z. Herewith $N_x + N_y + N_z = N$. So a local disturbance in the lattice creates the situation that [5] interpreted as negative energy but if we look at the whole system, there is no reason to assume negative temperatures below 0 K.

2.4.4 A CLUSTER OF ELECTRONS

A series of reports informed about observation of electron droplets [6–11]. Those droplets were generated through electric discharges. Interesting studies of charge droplets punching various materials were carried out by Shoulders and Shoulders [47].

Kukhtarev and Kukhtareva [12] carried out an experiment in which the formation of electron droplets was observed after illumination of a $LiNbO_3$ crystal by a focused laser beam (CW green laser, $\lambda_{\text{laser}} = 532$ nm, $P = 100$ mW). In the course of the experiments, we observed a usual recording of holographic gratings. An interference pattern was formed between the pump laser beam and the scattered waves producing moving space-charge waves inside the crystal. Due to the electro-optic effect these space-charge waves modulated the refractive index, which resulted in the formation of holographic gratings. Thus, the pump laser beam diffracted on the holographic gratings visualizing the space-charge waves.

In addition we observed a very unusual phenomenon. Owing to the illumination of the crystal, a photon bunch induced electron emission in the impact area of the crystal boundary. The emitted electrons manifested themselves via an emergence of specular reflection spots (Fig. 2.10). An analysis showed that those enigmatic droplets had the size of about 100 μm and each droplet included around 10^{10} electrons. Those bright droplets slowly moved in the space along the crystal surface.

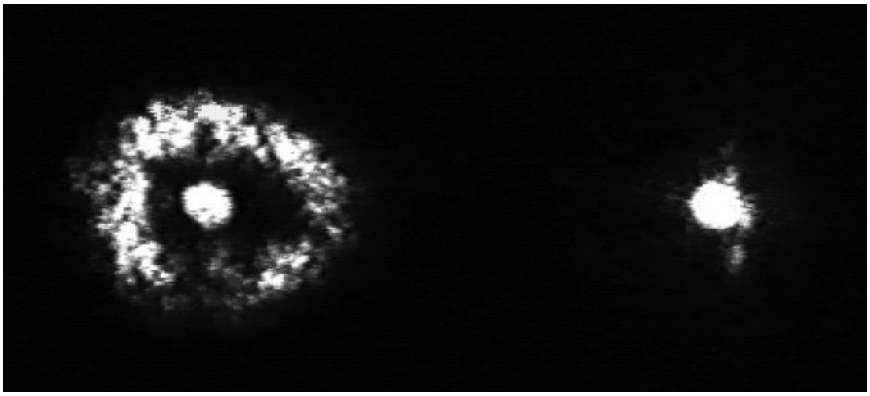

FIGURE 2.10 Left image: Enhanced back-reflected scattering from the surface of the ferroelectric crystal $LiNbO_3$ covered with a thin metal film as seen on the screen. Right image: The specular reflected beam with the droplet.

Free electrons have never been observed at a velocity smaller than 10^5 m s^{-1}. At the same time in the experiment studied a droplet of electrons had a velocity only about 0.5 cm s^{-1}. But how naked electrons could gather together in such a small space? A 10^{10} electrons in a droplet with a radius of 50 μm results in an electron density of about 10^{24} m^{-3}, which means that the mean distance between electrons $\overline{r} \approx 10^{-8}$ m. Hence the repulsion energy between nearest electrons in the droplet becomes

$$E_{\text{repulsion}} = \frac{e^2}{4\pi\varepsilon_0 \overline{r}} \approx 2.3\times10^{-20} \text{ J} \tag{55}$$

where e is the elementary electric charge and ε_0 is the dielectric constant. It seems the repulsion energy (the Eq. (54)) should lead to the scattering of electrons with the same kinetic energy, $E_{\text{repulsion}} = E_{\text{kinetic}} = m\upsilon^2/2$, which gives the electron velocity $\upsilon \approx 2\times10^5$ m×s^{-1}. However, electrons were not released from the droplets. So, they are strongly kept by a mysterious force!

To unravel the mystery, we must assume that the echo pulse transferred not only acoustic waves by also a flow of inertons knocked out from the vibrating crystal lattice of $LiNbO_3$. In the vicinity of the surface of the crystal photoelectrons absorbing inertons significantly change their behavior. Namely, the inerton field ties the electrons together. This means that in the droplet electrons are characterized by two kinds of interactions: the Coulomb repulsion (55) and an elastic interaction caused by the overlapping of electrons' inerton

clouds (or wave ψ-functions in terms of the conventional quantum mechanical formalism). The absorption of inertons strengthens the elastic interaction between electrons, which is able to compensate the electrons' Coulomb repulsion.

Let us introduce a dimensionless distance x. Then the repulsive paired potential for electrons can be rewritten as

$$V^{\text{rep.}} = \frac{1}{4\pi\varepsilon_0}\,\frac{e^2}{\overline{r}\,x} \tag{56}$$

The elastic interaction of electrons through the inerton field may be presented in the form of a typical harmonic potential

$$V^{\text{att.}} = \tfrac{1}{2} m\omega^2 \cdot (\delta\overline{r}\ x)^2 \tag{57}$$

where m is the mass of an electron in the droplet, ω is the cyclic frequency of its oscillations and $\delta\overline{r}$ is the amplitude of the electron displacement from its equilibrium state (note that this amplitude $\delta\overline{r}$ is directly connected with the de Broglie wavelength of the electron, $2\,\delta\overline{r} = \lambda$).

Then calculating the functions a (39) and b (40) and substituting them into the action (Eq. (38)) we obtain

$$S \approx \left(\frac{3e^2}{8\pi\varepsilon_0\,\overline{r}\,k_{\text{B}}\Theta}\,N^{2/3} - \frac{3\,m\,\omega^2\,\delta\overline{r}^{\,2}\,N^{5/3}}{10\,k_{\text{B}}\Theta} \right) N^2 \tag{58}$$

The minimum of action (Eq. (58)) is reached at the solution of the equation $\partial S / \partial N = 0$ (if the inequality $\partial^2 S / \partial N^2 > 0$ holds). The corresponding solution is

$$N \approx \frac{20}{11}\,\frac{e^2/(4\pi\varepsilon_0\,\overline{r})}{\tfrac{1}{2} m\omega^2\,\delta\overline{r}^{\,2}} \tag{59}$$

Therefore the quantity of electrons involved in a droplet is determined by the ratio of repulsive and attractive paired potentials.

The value of the frequency $2\pi\omega$ can be estimated as 1 MHz, as evidenced by radiosignals recorded from droplets. Then substituting numerical values of all the parameters into Eq. (59), we will find that the quantity $N \approx 10^{10}$ of electrons in a droplet is reached at a non-realistically large size of the amplitude $\delta\overline{r} \sim 10^{-5}$ m of oscillations of electrons near their equilibrium positions. However, the conflict can be easily overcome, if we introduce an effective mass m^* for the electron and put a reasonable size $\delta\overline{r} \approx 10^{-10}$ to 10^{-9} m for

the amplitude of the electron oscillations. The quantity $N \approx 10^{10}$ is satisfied when $m^* \approx 2 \times (10^{-22}$ to $10^{-24})$ kg, which exceeds the rest mass of electrons millions of times.

Hence the variation in the mass of electrons allows us to resolve the problem of the electron droplet stability.

2.5 CASIMIR EFFECT

Investigators studying the Casimir effect are confident that Casimir forces can drive the operation of nanomachinery and therefore such research is very important [48]. The majority of researchers associate these forces with the fractal energy $E_0 = \frac{1}{2}\hbar\omega$, or zero-point energy, which is treated as the inner energy of vacuum fluctuations of the electromagnetic field [49]. As a result all mechanical effects observable in mesoscopic physics are connected with effects occurring in the physical vacuum itself. In quantum field theory, the London – van der Waals forces, Casimir-Polder forces and the Casimir and Lifshitz forces are physical forces arising from a quantized field.[1] considered two conducting square plates with the size $\mathcal{L} \times \mathcal{L}$ separated by a distance *a*. One plate is movable and in the first situation the distance *a* is small and in the second situation it is large.

Casimir [1] considered two

$$\delta E = (\tfrac{1}{2}\sum_i \hbar\omega_i)_I - (\tfrac{1}{2}\sum_i \hbar\omega_i)_{II} \tag{60}$$

between two summations that extend over all possible resonance frequencies in the vacuum cavity confined by these two plates. The geometric size of the cavity $0 \le x \le \mathcal{L}$, $0 \le y \le \mathcal{L}$ and $0 \le z \le a$ determines its possible vibrating modes: $k_x = n_x \pi / \mathcal{L}$, $k_y = n_y \pi / \mathcal{L}$ and $k_z = n_z \pi / a$. To every k_x, k_y, k_z correspond two standing waves. In an explicit form these standing electromagnetic waves spontaneously excited in vacuum have the form

$$\mathbf{A} = \sum_k c\sqrt{\frac{\pi\hbar}{\omega\mathcal{L}^2}}\,\mathbf{e}(\mathbf{k}) \times \left\{ A_k e^{-(\omega t - \mathbf{kr})} + A_k^+ e^{(\omega t - \mathbf{kr})} \right\} \tag{61}$$

For large $\mathcal{L}$ wave numbers k_x and k_y can be regarded as continuous variables. Then Casimir presented the difference δE (60) in an integral form, which allowed him to obtain the final result – an attractive energy between the two plates:

$$\delta E / \mathcal{L}^2 = -\hbar c \frac{\pi^2}{24 \times 30} \cdot \frac{1}{a^3} \tag{62}$$

The calculated result of Eq. (62) was verified experimentally by different researchers. Moreover, the Casimir effect occurs also in the case of dielectrics [50], which points to its universality. Nowadays both theorists and experimentalists continue to intensively study the Casimir effect. Theoreticians have been developing complicated generalized mathematical approaches based on fluctuations of electromagnetic field, virtual photons and other things that would appear from the zero-point energy and the physical vacuum in general [2, 3, 48–50].

At the same time Refs. [51] and [52] presented a very different viewpoint describing the same phenomenon, i.e. the attraction of two plates. The starting point is the consideration of a scalar field of mass m that satisfies the wave equation $(\nabla^2 + k^2)\phi(x) = 0$. The Casimir energy is written as an integral over the difference between the density of states $\delta\rho(k)$ in a domain of conducting planes and the vacuum,

$$\delta E = \tfrac{1}{2}\hbar \int_0^\infty dk\, \omega(k) \frac{2k}{\pi} \operatorname{Im} \int_D d^3x\, \tilde{G}(x,\ x,\ k + i\varepsilon) \tag{63}$$

where $\omega = \sqrt{c^2k^2 + m^2c^4/\hbar^2}$ and $\tilde{G} = G - G_0$ is the difference between the Green's function in the background of conducting plates and the Green's function in vacuum. To resolve the equation (63), [51] chose the Green's function typical for classical geometric optics when *G* is defined by the sum over optical paths, which includes a combination of abstract factors used in classical ray optics. Then the mass *m* is approaching zero and they finally acquire Casimir's result (62).

Thus, the Casimir effect can be considered without reference to zero point energies. It can be originated from relativistic, quantum forces between fluctuations of charges and currents in borderline material plates [52].

We can further develop the Jaffe's view; namely, materialize his fictitious scalar massive field $\phi(x)$ and combining it with the mathematical method suggested by Casimir [1].

In the previous sections, we introduced submicroscopic mechanics starting from the constitution of the real space in the form of the tessel-lattice. It has been shown that the motion of an object in the tessel-lattice leads to the

generation of inertons around it. In particular, neutral atoms and ions oscillating at their equilibrium positions in a solid generate inertons. Acoustic vibrations of entities in condensed matter produce long inerton waves that spread out of the matter as standing inerton waves. These are standing inerton waves of a body that form its Newtonian gravitational potential [32, 34, 37].

A linear spectrum of acoustic phonons breaks at the Debye frequency. At higher frequencies the dispersion relation is no longer linear (Fig. 2.11.). Round the edge of the Brillouin zone the spectrum of large wave numbers k becomes increasingly closer to discrete, because the distance between the wave numbers grows towards the edge of the Brillouin zone [53].

Therefore, since the spectrum of phonons at the edge of the Brillouin zone is specific, we may anticipate that the edge phonons will contribute to the inerton spectrum distinctively as well. Especially it can be justified in the case of near-surface atoms of the material body. Near-surface atoms may have a more obvious discrete spectrum at the edge of the Brillouin zone than the bulk atoms and the difference of these spectra may give an additional distribution of inertons out of the body's surface.

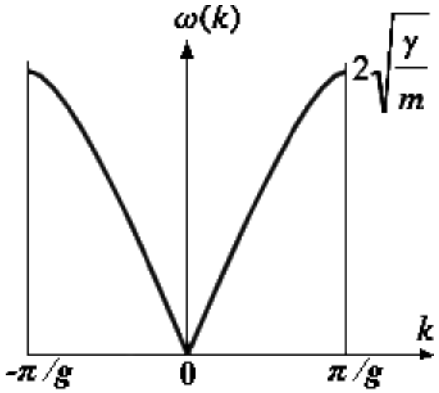

FIGURE 2.11 Spectrum of acoustic phonons that is destroyed near the end of the Brillouin zone.

Indeed, if the amplitude of a vibrating atom is δr, which is the atom's de Broglie wavelength λ, than the amplitude of its inerton cloud is $\Lambda = \lambda c / \upsilon$ (20), where the phase speed is $\upsilon = (2g / \pi) \times \sqrt{\gamma / m}$ (for 1D chain). For example, in the case of gold, its force constant γ may be estimated as varying from 4 to 9 N×m^{-1} [54]. Let us put $\gamma = 4$ N×m^{-1}. The lattice constant of gold

is $g = 4.08\times10^{-10}$ m; the mass of the atom of gold is $m_{\mathrm{Au}} = 3.27\times10^{-25}$ kg. Knowing these parameters, we valuate the phase velocity as $\upsilon \approx 9.08\times10^{2}$ m×s^{-1}. Then the amplitude of vibrations of the pair of atoms at the edge of the Brillouin zone, that is, the atom's de Broglie wavelength, becomes $\delta r \equiv \lambda = h/(m_{\mathrm{Au}}\upsilon) = 2.23\times10^{-12}$ m. The appropriate amplitude of the atom's inerton cloud is $\Lambda = \lambda\, c/\upsilon = 0.74$ μm. This value of Λ should be slightly lengthened owing to contributions on the side of other discrete modes and the thermal smearing. Nevertheless, the estimated value of Λ accounts for an order of the radius of the boundary effects that can specifically manifest themselves in the vicinity of the body.

It is intuitively clear these boundary inerton effects are logically linked to the Casimir effect. To proof this, we need to calculate the energy of attraction caused by short wave inertons.

Let us imagine a rectangular cuboid whose base $\mathcal{L}\times\mathcal{L}$ is located on the surface of a material body and it sticks outward having the height *a*. Let another cuboid with the same size be disposed inside the material body. What is the difference in the vibrating inerton energy for these two cuboids? Then we follow the computational scheme proposed by Casimir [1]:

$$\delta E = \hbar\omega \frac{1}{(\pi/\mathcal{L})^2}\frac{1}{(\pi/a)} \times\left\{\sum_{n=0}^{\infty}\int_0^{\infty}\int_0^{\infty}\sqrt{k_x^2+k_y^2+\frac{\pi^2n^2}{a^2}}\,dk_x dk_y - \int_0^{\infty}\int_0^{\infty}\int_0^{\infty}\sqrt{k_x^2+k_y^2+\frac{\pi^2n^2}{a^2}}\,dk_x\,dk_y\,dn\right\}. \quad (64)$$

Now turn to polar coordinates ($\sqrt{k_x^2+k_y^2}=\kappa$)

$$\delta E = \hbar\, 2\pi v a\,\frac{\mathcal{L}^2}{\pi^2}\frac{1}{\pi}\left\{\sum_{n=0}^{\infty}\frac{\pi}{2}\int_0^{\infty}\sqrt{\kappa^2+\frac{\pi^2n^2}{a^2}}\,\kappa d\kappa - \frac{\pi}{2}\int_0^{\infty}\int_0^{\infty}\sqrt{\kappa^2+\frac{\pi^2n^2}{a^2}}\,\kappa d\kappa dn\right\}$$

$$= \hbar c\,\pi\frac{\mathcal{L}^2}{\pi^2}\left\{\sum_{n=0}^{\infty}\int_0^{\infty}\sqrt{\frac{a^2\kappa^2}{\pi^2}+n^2}\;\frac{\pi}{a}\kappa d\kappa - \int_0^{\infty}\int_0^{\infty}\sqrt{\frac{a^2\kappa^2}{\pi^2}+n^2}\;\frac{\pi}{a}\kappa d\kappa dn\right\} \quad (65)$$

Let us introduce a new variable, $u = \kappa^2 / (\pi / a)^2$, which changes Eq. (65) to the form

$$\delta E = \hbar c \pi \frac{\mathcal{L}^2}{\pi^2} \cdot \frac{1}{2} \left(\frac{\pi}{a} \right)^3 \left\{ \sum_{n=0}^{\infty} \int_0^{\infty} \sqrt{u + n^2}\ du - \int_0^{\infty} \int_0^{\infty} \sqrt{u + n^2}\ du\, dn \right\}, \tag{66}$$

where under the integrands we have only dimensionless variables. Now we need to get rid of divergences in the integrals. Following Ref. [1], we introduce a cutoff function $f(k/k_{\rm m})$, which equals to 1 when $k << k_{\rm m}$, and 0 when $k >> k_{\rm m}$. Besides, imputing a new variable, $w = \sqrt{u + n^2}$, we get instead of Eq. (66)

$$\begin{aligned} \delta E &= \frac{\hbar c \pi^2 \mathcal{L}^2}{2a^3} \cdot \left\{ \sum_{n=0}^{\infty} \int_n^{\infty} 2w^2\ f\left(\frac{\pi w / a}{k_{\rm m}} \right) dw - \int_0^{\infty} \int_n^{\infty} 2w^2 f\left(\frac{\pi w / a}{k_{\rm m}} \right) dw\, dn \right\} \\ &= \frac{\hbar c \pi^2 \mathcal{L}^2}{a^3} \left\{ \sum_{n=0}^{\infty} F(n) - \int_0^{\infty} F(n)\, dn \right\}, \end{aligned} \tag{67}$$

where

$$F(n) = \int_0^{\infty} w^2 f[\pi w / (a k_{\rm m})]\, dw \tag{68}$$

If $F(n)$ and all its derivatives tend to 0 as $n \to \infty$, the curly braces in Eq. (67) can be presented as follows [55].

$$\sum_{n=0}^{\infty} F(n) - \int_0^{\infty} F(n)\, dn = \frac{1}{2} F(0) - \frac{1}{12} F'(0) + \frac{1}{24 \cdot 30} F'''(0) + \ldots \tag{69}$$

Since $F'(n) = -n^2 f[\pi n / (a k_{\rm m})]$, $F''(n) = -2n f[\pi n / (a k_{\rm m})]$, $F'''(n) = -2 f[\pi n / (a k_{\rm m})]$ and the function f is the step function (zero and unity), it is reasonable to put here its mean value, $f = \langle f \rangle = 1/2$. Then we get: $F(0) = 0$, $F(0) = 0$, $F(0) = -1$. Substituting these values into the right-hand side of Eq. (69) we obtain the result: $-1/(24 \cdot 30)$. Substituting this value into the expression for δE (the Eq. (67)), we immediately arrive at the Casimir outcome (the Eq. (62)).

Thus, the Casimir attraction energy is caused by the inerton deformation of space in the vicinity of the plate's surface. Inertons carry mass and hence they induce a peculiar distribution of the gravitational potential around a body. Shortwave inertons generated by vibrating atoms at the edge of the

Brillouin zone are responsible for the gravitational potential energy (the Eq. (62)), which produces a gravitational force $\mathcal{F} = \hbar c \pi^2 / (240 a^4)$ per square unit of the area. Longwave inertons generated by atoms in the acoustic spectrum induce the conventional Newtonian gravitational potential. Hence, at a short distance (about 1 μm or so) the gravitational potential is proportional to $1/r^3$ and at macroscopic distances it is proportional to $1/r$.

2.6 CONCLUDING REMARKS

In this chapter, we have shown that the real physical space is constructed as the tessel-lattice of primary topological balls, superparticles of the nature. In the tessel-lattice particles are determined as local stable deformations. The motion of a particle generates a cloud of Poincaré like excitations around the particle, which were named *inertons*. It has been argued that a particle together with its cloud of inertons emerges in conventional quantum mechanics as an abstract construction called the wave ψ-function. These particle's inertons carry both particle's inert and gravitational properties.

The inerton field, as well as the electromagnetic field, are basic fields of the nature. The inerton field is able to give a deeper insight into fundamental nature of things playing an important role in quantum physics, chemical physics, biochemistry, biophysics, and condensed matter. The inerton field assembles neutral and charged particles, changes physical chemical properties of substance, such as viscosity, density, microhardness, conductivity, thermodynamic potentials, etc.

There are a large variety of nanosystems and in some of them inerton effects are quite significant. We have to mention also the recent finding of a new bosonic quasi-particle named 'bondon,' which aggregates distant quantum particles [56, 57]. What is the reason for coupling of distant quantum particles? We may suggest that it is through the particles' clouds of inertons. Because the wave ψ-function of such an aggregation allows for a separate study of the ψ-function's core and its tail [58].

Fuchs et al. [59] presented a measurement of the excited state spin levels of a single Nitrogen-vacancy center in diamond. It was found that strain plays a critical role in the spin dynamics significantly influencing transverse anisotropy and hyperfine splitting. Therefore, the spin levels can be adjusted through strain engineering. Not only magnetic and electric field, but also an inerton field can induce strain. Hence the inerton field also is able to control high-speed physical reactions, the more so that it is able to deeper penetrate materials in comparison with the electromagnetic field.

In nanophotonics, optical properties of thin films are determined by diffractive elements, which represent a quantum confinement needed to tune the properties of electrons and photons together [60]. An inerton field is able to affect the absorption cross section of quantum dots, which can be used in nanophotonics. In fact the author of Ref. [61] has shown that at a submicroscopic level inertons are responsible for the phenomenon of diffraction.

A few research teams could generate a hydrogen atom of the nuclear size. This phenomenon was called differently by them: 'hydrex' (for hydrogen) and 'deutrex' (for deuteron) [62–65] 'hydrino' [66–71], and 'pseudoneutron' [72–74]. To understand the principles of operation of such an exotic system, the researchers suggest new ideas, which seem very different in each special case. Nevertheless, from the author's point of view, these nano- and submicroscopic systems can be unified and accounted for in the framework of the deterministic submicroscopic concept of physics, which includes inerton field as a basic field of nature. Besides, though a number of experiments were conducted in the area of low energy nuclear reaction, so far still no reasonable theory was reported [75]. A theory of could fusion can be developed on the basis of the present submicroscopic concept, which will open a gateway for optimization of crucial experiments in this important area of research.

KEYWORDS

- **Casimir effect**
- **electromagnetic field**
- **frustrated matter**
- **quasi-particles**
- **space excitation**
- **space particles' gravitation**
- **inerton field effects**

REFERENCES

1. Casimir, H. B. G. (1948). On the attraction between two perfectly conducting plates, *Proc. K. Ned. Akad. Wet*. 51, 793–795.
2. Genet, C., Intravaia, F., Lambrecht, A., Reynaud, S. (2004). Electromagnetic vacuum fluctuations, Casimir and Van der Waals forces, *Ann. Fond. L. de Broglie* 29, 311–328; arXiv:quant-ph/0302072.
3. Denardo, B. C., Puda, J. J; Larraza, A. S. (2009). A water wave analog of the Casimir effect, *Americ. J. Phys.* 77(12), 1095–1101.

4. Lambrecht, A., Reynaud, S. (2011). Casimir Effect: Theory and Experiments, arXiv:1112.1301 [quant-ph].
5. Braun, S., Ronzheimer, J. P., Schreiber, M., Hodgman, S. S., Rom, N., Bloch, I., Schneider, U. (2013). Negative absolute temperature for motional degrees of freedom, Science 339, no. 6115, 52–55; arXiv:1211.0545 [cond-mat.quant-gas].
6. Beckmann, P. (1990). Electron clusters, *Galilean Electrodynamics*, Sept./Oct. 1(5), 55–58.
7. Shoulders, K. R. Energy conversion using high charge density, U.S. patent 5,018,180, May, 1991.
8. Shoulders, K., Shoulders, S. (1996). Observations of the role of charge clusters in nuclear cluster reactions, *J. New Energy* 1(3), Fall.
9. Ziolkowski, R. W., Tippett, M. K. (1991). Collective effect in an electron plasma system catalyzed by a localized electromagnetic wave, *Phys. Rev. A* 43(6), pp. 3066–3072.
10. Mesyats, G. A. (1996). Ecton processes at the cathode in a vacuum discharge, Proc. XVIIth Int. Symposium on Discharges and Electrical Insulation in Vacuum, Berkeley, CA, July 21–26; pp. 721–731.
11. Lisitsyn, I., Akiyama, H., Mesyats, G. A. (1998). Role of electron clusters - ectons - in the breakdown of solids dielectrics, *Phys. Plasma* 5(12), 4484–4487.
12. Krasnoholovets, V., Kukhtarev, N., Kukhtareva, T. (2006). Heavy electrons: Electron droplets generated by photogalvanic and pyroelectric effects, *International Journal of Modern Physics B* 20(16), 2323–2337; arXiv:0911.2361 [quant-ph].
13. Vernadsky, V. On the states of physical space, *21th Century Science and Technology*, Winter 2007–2008 Issue, pp. 10–22, http://www.21stcenturysciencetech.com/Articles%202008/States_of_Space.pdf
14. Perez, A. (2008). Spin foam models for quantum gravity, *Class. Quant. Grav*. 20**,** R43.
15. Preparata, G. (1995). Quantum gravity, the Planck lattice and the standard model, arXiv:hep-th/9503102.
16. Konushko, V. I. (2011). Granular space and the problem of large numbers, *J. Mod. Phys.* 2, 289–300.
17. Wilczek, F. (2009). What is space? *Physics @MIT* 30, http://web.mit.edu/physics/people/faculty/docs/wilczek_space06.pdf
18. Bounias, M., Krasnoholovets, V. (2003). Scanning the structure of ill-known spaces: Part 1. Founding principles about mathematical constitution of space, *Kybernetes: The Int. J. Systems and Cybernetics* 32, no. 7/8, 945–75, Eds.: L. Feng, B. P. Gibson and Yi Lin; also arXiv:physics/0211096.
19. Schwartz, L. (1991). *Analyse I: théorie des ensembles et topologie* (Hermann, Paris), p. 24.
20. James, G., James, R. C. (1992). *Mathematics Dictionary* (Van Nostrand Reinhold, New York), pp. 267–68.
21. Bounias, M., Krasnoholovets, V. (2003). Scanning the structure of ill-known spaces: Part 2. Principles of construction of physical space, *Kybernetes: The Int. J. Systems and Cybernetics* 32, no. 7/8, 976–1004, Eds.: L. Feng, B. P. Gibson and Yi Lin; also arXiv:physics/0212004.
22. Bounias, M., Krasnoholovets, V. (2003). Scanning the structure of ill-known spaces: Part 3. Distribution of topological structures at elementary and cosmic scales,

Kybernetes: The Int. J. Systems and Cybernetics 32, no. 7/8, 1005–20, Eds.: L. Feng, B. P. Gibson and Yi Lin; also arXiv:physics/0301049.
23. Krasnoholovets, V., Ivanovsky, D. (1993). Motion of a particle and the vacuum, *Phys. Essays* 6(4), 554–563; arXiv:quant-ph/9910023.
24. Krasnoholovets, V. (1997). Motion of a relativistic particle and the vacuum, *Phys. Essays* 10(3), 407–416; arXiv:quant-ph/9903077.
25. Poincaré, H. Sur la dynamique de l'électron, *Comptes Rendus* (1905). 140, pp. 1504–1560, *Rendiconti del Circolo matematico di Palermo* (1906). 21, 129–176 (1906); also: Oeuvres, t. IX, pp. 494–550 (and also in Russian translation: *Selected Transactions*, Ed.: N. N. Bogolubov (Nauka, Moscow, 1974), 3, 429–486).
26. De Broglie, L. Recherches sur la théorie des quanta, *Ann. De Phys*., 10^{e} série, t. III (Janvie-Février 1925); translation by A.F. Kracklauer: *On the theory of quanta*, Lulu. com; Morrisville, NC; 2007 (ISBN: 978–1-84753–358–6).
27. De Broglie, L. (1987). Interpretation of quantum mechanics by the double solution theory, *Ann. de la Fond. L. de Broglie* 12, 399–421.
28. Born, M. Das Adiabatenprinzip in der Quantenmechanik, *Zeitschrift für Physik* (1926). 40, 167–192.
29. Born, M. The statistical interpretation of quantum mechanics. *Nobel Lecture*, December 11, 1954.
30. Krasnoholovets, V. (2002). Submicroscopic deterministic quantum mechanics, *Int. J. Computing Anticipatory Systems* 11, 164–179; arXiv:quant-ph/0109012.
31. De Broglie, L. *Les incertitudes d'Heisenberg et l'interprétation probabiliste de la méchanique Ondulatoire* (Gauthier-Villars, Bordas, Paris, 1982); Chapter 2, sect. 4.
32. Krasnoholovets, V. (2010). Inerton fields: Very new ideas on fundamental physics, *American Inst. Phys. Conf. Proc*. - December 22, vol. 1316, 244–268. *Search for fundamental theory: The VII International Symposium Honoring French Mathematical Physicist Jean-Pierre Vigier* (12–14 July 2010, Imperial College, London), Eds.: R. L. Amoroso, P. Rowlands and S. Jeffers; doi:10.1063/1.3536437.
33. Krasnoholovets, V. (2010). Variation in mass of entities in condensed media, *Applied Physics Research* 2(1), 46–59; http://www.ccsenet.org/journal/index.php/apr/article/view/4287.
34. Krasnoholovets, V. (2008). Reasons for the gravitational mass and the problem of quantum gravity. In *Ether, spacetime and cosmology. Vol. 1. Modern ether concepts and geometry*; Duffy, M., Levy, J., Krasnoholovets, V., Eds., PD Publications: Liverpool, Vol. 1; pp. 419–450; arXiv: 1104.5270 [physics.gen-ph].
35. Krasnoholovets, V. (2009). On microscopic interpretation of phenomena predicted by the formalism of general relativity, in Ether space-time and cosmology, Vol. 2: New insights into a key physical medium. Eds.: M. C. Duffy and J. Levy (Publisher: C. Roy Keys Inc. Apeiron, 2009); also: *Apeiron* 16(3), 418–438, http://redshift.vif.com/JournalFiles/V16NO3PDF/V16N3KRA.pdf.
36. Krasnoholovets, V. (2013). On the gravitational time delay effect and the curvature of space, *Int. J. Computing Anticipatory Systems. Proceedings of the Tenth International Conference CASYS'11 on Computing Anticipatory Systems, Liège, Belgium, August 8–13, 2011, D. M. Dubois (Ed.),* Publ. by CHAOS, 2012. ISSN 1373–5411.
37. Krasnoholovets, V. (2011). Dark matter as seen from the physical point of view, *Astrophys. Space Science* 335(2), 619–627.

38. Krasnoholovets, V. (2009). Inerton fields: A new approach in fundamental physics, *Proc. Bath Royal Literary and Scientific Institution*, Vol. 11, Sep 2006-Aug 2007, Bath Royal Literary and Scientific Institution, Bath, pp. 266–272 (ISSN 1465–8496).
39. Krasnoholovets, V., Lev, B. (2003). Systems of particles with interaction and the cluster formation in condensed matter, *Cond. Matt. Phys*. 6, 67–83; arXiv:cond-mat/0210131.
40. Khachaturian, A. G. (1974). *The theory of phase transitions and the structure of solid solutions*, Nauka, Moscow, p. 100 (in Moscowian).
41. Melker, A. I. (2009). Potentials of interatomic interaction in molecular dynamics, *Rev. Adv. Mater. Sci.* 20, 1–13.
42. Krasnoholovets, V., Tomchuk, P. M., Lukyanets, S. P. (2003). Proton transfer and coherent phenomena in molecular structures with hydrogen bonds, in *Advances in Chemical Physics*, Vol. 125, Eds.: Prigogine, I. and Rice, S. A. John Wiley & Sons, Inc.
43. Krasnoholovets, T., Tane, J.-L. (2006). An extended interpretation of the thermodynamic theory, including an additional energy associated with a decrease in mass, *Int. J. Simulation and Process Modeling* 2(1/2), 67–79; arXiv:physics/0605094.
44. Tane, J.-L. (2009). Unless connected to relativity, the first and second laws of thermodynamics are incompatible, arXiv:0910.0781 [physics.gen-ph].
45. Tane, J.-L. (2012). A simple illustration of the need for relativity in thermodynamics, *The General Science J*. http://gsjournal.net/Science-Journals/Research%20Papers-Relativity%20Theory/Download/4312 .
46. Zhang, S. (2012). Entropy: A concept that is not a physical quantity, *Phys. Essays* 25(2), 172–176.
47. Shoulders, K., Shoulders, S. (1999). Charge clusters in action, http://www.svn.net/krscfs/Charge%20Clusters%20In%20Action.pdf
48. Milton, K. A. (2011). Resource Letter VWCPF-1: Van der Waals and Casimir-Polder forces arXiv: 1101.2238 [cond-mat.other].
49. Milonni, P. W. (1994). *The quantum vacuum. An introduction to quantum dynamics*. Academic Press.
50. Bordag, M., Mohideen, U., Mostepanenko, V. M. (2001). New developments in the Casimir effect, *Physics Reports* 353, 1–205.
51. Jaffe, R. L., Scardicchi, A. (2004). The Casimir Effect and Geometric Optics, *Phys. Rev. Lett*. 92: 070402, arXiv:quant-ph/0310104.
52. Jaffe, R. L. (2005). The Casimir effect and the quantum vacuum, *Phys. Rev. D* 72(2), 021301, arXiv:hep-th/0503158.
53. Kosevich, A. M. (2005).*The crystal lattice: Phonons, solitons, dislocations, superlattices*. Willey-VCH Verlag GmbH & Co. KGaA, Weinheim, p. 20.
54. Valkering, A. M. C., Mares, A. I., Untiedt, C., Babaei Gavan, K., Oosterkamp, T. H., van Ruitenbeek, J. M. (2005). A force sensor for atomic point contacts, *Rev. Scientific Instruments* 76, 103903 (5 pages).
55. Kac, V., Cheung, P. (2001). *Quantum Calculus*, Springer; p. 93 and 87.
56. Putz, M. V. (2010). The bondons: The quantum particles of the chemical bond, *Int. J. Mol. Sci.* 11, 4227–4256.
57. Putz, M. V., Ottorino, O. (2012). Bondonic characterization of extended nanosystems: Application to graphene's nanoribbons, *Chem. Phys. Lett.* 548, 95–100.

58. Putz, A.-M; Putz, V. M. (2012). Spectral inverse quantum (spectral-IQ) method for modeling mesoporous systems: application on silica films by FTIR, *Int. J. Mol. Sci.* 13, 15925–15941.
59. Fuchs, G. D., Dobrovitski, V. V., Hanson, R., Batra, A., Weis, C. D., Schenkel, T., Awschalom, D. D. (2008). Excited-State Spectroscopy Using Single Spin Manipulation in Diamond, *Phys. Rev. Lett.* 101, 117601 [4 pages].
60. Flory, F., Escoubas, L., Berginc, G. (2011). Optical properties of nanostructured materials: a review, *J. Nanophoton.* 5(1), 052502. http://nanophotonics.spiedigitallibrary.org/article.aspx?articleid=1226099
61. Krasnoholovets, V. (2010). Sub microscopic description of the diffraction phenomenon, *Nonlin. Optics, Quant. Optics* 41(4), 273–286.
62. Dufour, J. (1993). Cold fusion by sparking in hydrogen isotopes, *Fusion Technol.* 24, 205–228.
63. Dufour, J., Foos, J., Millot, J. P., Dufour, X. (1997). Interaction of palladium/hydrogen and palladium/deuterium to measure the excess energy per atom for each isotope, *Fusion Technol.* 31, 198–209.
64. Dufour, J., Murat, D., Dufour, X., Foos, J. (2000). Hydrogen triggered exothermal reaction in uranium metal, *Phys. Lett. A* 270(5), 254–264.
65. Dufour, J., Murat, D., Dufour, X., Fos, J. (2004). Exothermic reaction induced by high density current in metals – Possible nuclear origin, *Ann. Fond. L. de Broglie* 29(3), 1081–1093.
66. Mills, R. L. (2002). The grand unified theory of classical quantum mechanics *Int. J. Hydrogen Energy* 27, 565–590.
67. Mills, R., Dhandapani, B., Greenig, N., He, J. (2000). Synthesis and characterization of potassium iodo hydride, *Int. J. Hydrogen Energy* 25(12), 1185–1203.
68. Mills, R., Dhandapani, B., Nansteel, M., He, J., Voigt, A. (2001). Identification of compounds containing novel hydride ions by nuclear magnetic resonance spectroscopy, *Int. J. Hydrogen Energy* 26(9), 965–979.
69. Mills, R., Nansteel, M., Ray, P. (2002). Argon-hydrogen-strontium discharge light source, *IEEE Transact. Plasma Sci.* 30(2), 639–653.
70. Mills, R. L., Ray, P., Dhandapani, B., Mayo, R. M., He, J. (2002). Comparison of excessive Balmer alpha line broadening of glow discharge and microwave hydrogen plasmas with certain catalysts, *J. Appl. Phys.* 92, 7008–7022.
71. Mills, R., Ray, P., Dhandapani, B., Good, W., Jansson, P., Nansteel, M., He, J., Voigt, A. (2004). Spectroscopic and NMR identification of novel hydride ions in fractional quantum energy states formed by an exothermic reaction of atomic hydrogen with certain catalysts, *Eur. Phys. J. App. Phys.* 28, 83–104.
72. Borghi, C., Giori, C., Dall'Ollio, A. A. (1993). Experimental evidence of emission of neutrons from cold hydrogen plasma, *American Institute of Physics (Phys. At. Nucl.)* 56(7).
73. Conte, E., Pieralice, M. (1999). An experiment indicates the nuclear fusion of the proton and electron into a neutron, *Infinite Energy* 4(23), 67.
74. Santilli, R. M. (2006). Confirmation of Don Borghi's experiment on the synthesis of neutrons from protons and electrons, Preprint IBR-EP-39 of 12–25–06; arXiv.org: physics/0608229.
75. Storms, E. (2007). *The science of low energy nuclear reaction. A comprehensive compilation of evidence and explanations about could fusion*, World Scientific.